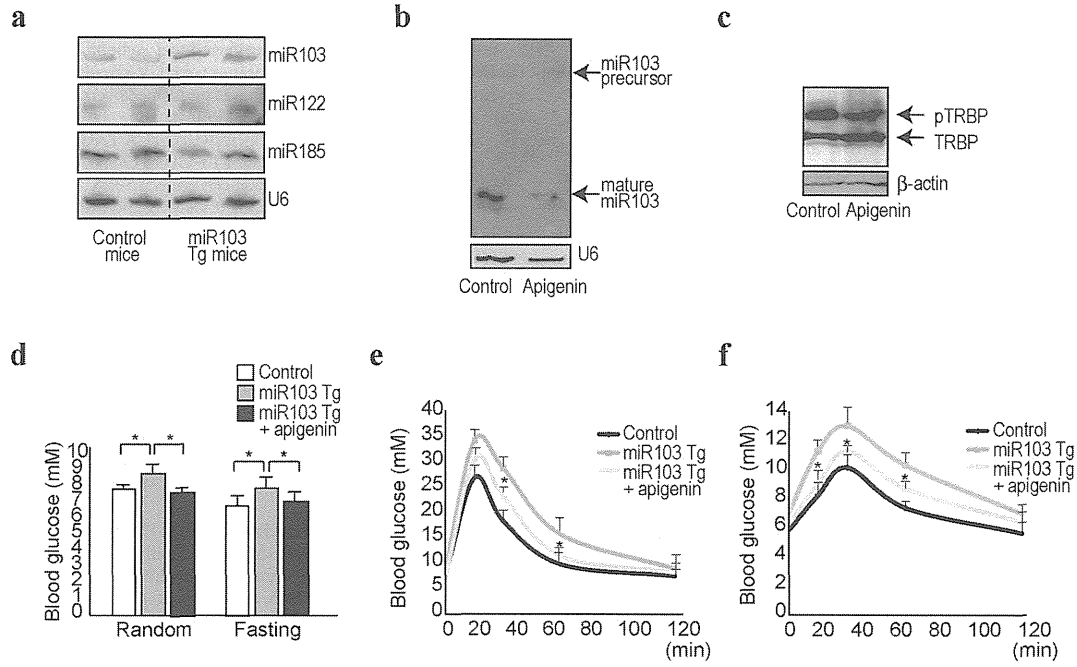


**Figure 4 | Apigenin improves glucose tolerance in miR103 transgenic mice.** (a), Expression levels of mature miR103, miR122, and miR185 in liver tissues of miR103 transgenic mice (miR103 Tg) were determined by Northern blotting. (b), Expression levels of mature miR103 and its precursor in liver tissues of miR10-transgenic mice treated with apigenin were determined by Northern blotting. Control (DMSO) or apigenin (40 mg/kg) was injected intraperitoneally daily for 14 days. Representative results from three independent mouse sets are shown. (c), Liver tissue homogenates from miR103 transgenic mice were separated using a phos-tag gel to determine the phosphorylation status of TRBP. Representative results from three independent mouse sets are shown. Full-length blot image is available in Supplementary Figure 5g. (d), Blood glucose levels were determined at random times or after 12 h fasting in control and miR103 transgenic (miR103 Tg) mice (n = 8 in each group). Data represent the means ± s.d. *, $p < 0.05$ (*t*-test). (e), (f), Glucose and pyruvate tolerance tests in control, miR103 transgenic (miR103 Tg), and miR103 transgenic with apigenin treatment (miR103 Tg + apigenin) mice (n = 6 in each group). Data represent the means ± s.d. *, $p < 0.05$ (*t*-test).

showed impaired glucose tolerance after an intraperitoneal glucose injection, apigenin treatment significantly suppressed these phenomena (Figure 4e). Similarly, while miR103 transgenic mice showed increased glucose production during an intraperitoneal pyruvate-tolerance test, apigenin treatment also suppressed these effects (Figure 4f). In addition, an increased number of small adipocytes and a decreased number of large adipocytes were observed in apigenin-treated miR103 transgenic mice (Supplementary Figure 3e and f). These results suggest that apigenin may have beneficial effects on pathological conditions in miR103 transgenic mice.

## Discussion

In this study, we demonstrated that apigenin (4′,5,7-trihydroxyflavone) has inhibitory effects on the maturation processes of a subset of miRNAs and subsequent miRNA function. These effects may be mediated through inhibition of TRBP phosphorylation, possibly through inhibition of Erk activation. These results suggest that apigenin may be utilized to improve miRNA-mediated pathogenic states, such as glucose tolerance, induced by the over-expression of miRNA103.

Bioactive substances, such as caffeine and polyphenols, have been reported to have pleiotropic physiological effects[3,20]. However, those phenomena are descriptive in most cases and the underlying mechanisms are largely unclear. Apigenin, which is present in many fruits and vegetables, also has diverse biological effects, including improvement of the cancer cell response to chemotherapy[21], tumorigenesis[13,22], modulating immune cell function[23], and anti-platelet activity[24]. In this study, we showed that apigenin inhibits TRBP phosphorylation and its related miRNA maturation through inhibition of MAPK Erk activation. This modulation of miRNA function by apigenin may account, at least in part, for its various reported biological effects.

Phosphorylation of TRBP is mediated by Erk[15]. We showed clear inhibition of Erk phosphorylation by apigenin. Although previous studies have reported the inhibition of Erk activation by apigenin[16–19], the underlying mechanisms were unknown. Because Erk has many biological functions in intracellular signaling, modulation of TRBP phosphorylation and miRNA expression induced by Erk inhibition through apigenin is likely a part of the phenotype. To clarify the biological function of apigenin, identification of molecules on which apigenin directly acts must be the next step.

Another important finding in this study was the impaired glucose tolerance observed in miR103 transgenic mice. Previous studies showed that recombinant adenoviruses expressing the miR103/107 family (only one nucleotide difference in miR103 and miR107 at position 21) and a gain of miR103/107 function by transient infection in mice was sufficient to induce impaired glucose homeostasis, and these miRNAs play a central role in insulin sensitivity[10]. In this study, we confirmed that constitutive expression of miR103 in mice resulted in impaired glucose tolerance and increased size of adipocytes. These mice may represent a new *in vivo* model of metabolic disorders and facilitate development of new drugs targeting impaired glucose tolerance. In fact, we found that apigenin reversed impaired glucose tolerance in miR103-transgenic mice. Because apigenin is one of the flavonoids and is present in high content in celery and parsley, intake of apigenin from foods or dietary supplements may have some favorable effects on glucose intolerance induced by overexpression of miRNA levels, even if it does not completely overcome impaired glucose tolerance.

Phosphorylated TRBP is not related to the maturation of all miRNAs, but rather a subset of miRNAs[15]. With this respect, apigenin may have favorable effects on the pathogenic status induced by overexpression or overfunction of the miRNAs to which phosphorylated TRBP is related. Maturation of miR122, a liver-specific miRNA, is at least partly regulated by apigenin, as shown in our study, its crucial function in cholesterol synthesis[11,25–28], and hepatitis c viral replication[29,30]. Therefore, apigenin may also have beneficial effects on these conditions. Other effects of apigenin on the pathological state may be necessary to reconsider from the point of view of overexpression or overfunction of specific miRNAs.

Simultaneously, one should be cautious about the modulation of miRNA function by apigenin. Because some miRNAs may have favorable effects on human health, apigenin might be harmful if it inhibits the maturation and function of such miRNAs. For example, inhibitory effects on tumor-suppressive miRNAs should be avoided. Caution regarding these issues is necessary and, in parallel, the biological functions of miRNAs in general should be further examined.

In summary, we showed that apigenin displays inhibitory effects on the phosphorylation of TRBP and its subsequent miRNA maturation and function through regulation of Erk activity. Decreasing miRNA function may be used for treatment of conditions induced by over-functioning of miRNAs. Moreover, clarifying the as-yet-undiscovered functions of bioactive substances is important. Similar strategies to those used here may also be applied to other bioactive substances whose effects have been reported but the mechanisms are as yet undetermined.

## Methods

**Cell culture.** The human hepatocellular carcinoma cell lines, Huh7 and Hep3B, were obtained from the Japanese Collection of Research Bioresources (JCRB, Osaka, Japan). All cells were maintained in Dulbecco's modified Eagle's medium supplemented with 10% fetal bovine serum.

**Reagents.** Caffeine, apigenin and chlorogenic acid were purchased from Wako Chemicals (Osaka, Japan). Procyanidin A2 and B2 were purchased from Indofine Chemical (Hillsborough, NJ) and ChromaDex (Irvine, CA). Caffeine, chlorogenic acid and procyanidin B2 were dissolved in water. Apigenin and procyanidin A2 were dissolved in dimethyl sulfoxide (DMSO). Caffeine, chlorogenic acid and procyanidin A2 and B2 were added at concentrations of 20 μM, 10 μM, 50 μg/mL, and 50 μg/mL, respectively, as reported previously[31–34]. Apigenin was used at 10 μM unless otherwise specified for *in vitro* studies, and 40 mg/kg was used for intraperitoneal injection daily for *in vivo* studies. An equal volume of DMSO only was used as a negative control.

**Mouse experiments.** Experimental protocols were approved by the Ethics Committee for Animal Experimentation at the Graduate School of Medicine, the University of Tokyo and the Institute for Adult Disease, Asahi Life Foundation, Japan and conducted in accordance with the Guidelines for the Care and Use of Laboratory Animals of the Department of Medicine, the University of Tokyo, and the Institute for Adult Disease, Asahi Life Foundation.

**Plasmids, transfection and dual luciferase assays.** Plasmids expressing miR122 and miR185 precursors and the corresponding firefly luciferase-based reporters have been described previously[8,35]. Plasmids expressing miRNA-103 precursors and the corresponding luciferase reporter were newly constructed according to protocols reported previously[8]. To determine MAPK pathway activity, SRE-driven luciferase was transfected, and dual luciferase assays were performed as described previously[9], with the exception that pGL4.74, a control plasmid containing *Renilla reniformis* (sea pansy) luciferase under control of the herpes simplex virus thymidine kinase promoter (Promega), was used as an internal control. Chemicals were added at 24 h and the reporter assays were done 48 h post-transfection. Constitutively active MEK1(DD) and dominant negative Erk(K/N) constructs with zeocin resistance genes were kindly provided by Prof. Takekawa (The Institute of Medical Sciences, the University of Tokyo)[36]. After transfection, the cells were selected with 6 μg/mL zeocin to establish cells stably expressing those constructs.

**Western blot analysis.** Protein lysates were prepared from cells or mouse liver tissues for immunoblotting analyses. Western blotting was performed as described previously[8]. Primary antibodies were purchased from Sigma (DGCR8, #SAB4200088; Dicer, #SAB4200087; TRBP2, #SAB4200111; β-actin, #A5441), Bethyl (KSRP, A302-021), Wako (Ago2, 015-22031), and Cell Signaling (Drosha, #D28B1; Phospho-Erk, #9101; Total Erk, #4695; myc-tag, #2276; Caveolin, #3267).

**Northern blotting of miRNAs.** Northern blotting of miRNAs was performed as described previously[9]. Briefly, total RNA was extracted using TRIzol Reagent (Invitrogen, Carlsbad, CA) according to the manufacturer's instructions. Ten micrograms of RNA were resolved in denaturing 15% polyacrylamide gels containing 7 M urea in 1× TBE and then transferred to a Hybond N+ membrane (GE Healthcare) in 0.25× TBE. Membranes were UV-crosslinked and prehybridized in hybridization buffer. Hybridization was performed overnight at 42°C in ULTRAhyb-Oligo Buffer (Ambion) containing a biotinylated probe specific for miR122 (CAA ACA CCA TTG TCA CAC TCC A), miR103 (TCA TAG CCC TGT ACA ATG CTG CT), miR185 (TCA GGA ACT GCC TTT CTC TCC A), and let-7g (AAC TGT ACA AAC TAC TAC CTC A), which had been heated to 95°C for 2 min. Membranes were washed at 42°C in 2× SSC containing 0.1% SDS, and the bound probe was visualized using a BrightStar BioDetect Kit (Ambion). Blots were stripped by boiling in a solution containing 0.1% SDS and 5 mM EDTA for 10 min prior to rehybridization with a U6 probe (CAC GAA TTT GCG TGT CAT CCT T).

**Quantitative RT-PCR analysis of miRNA expression.** To determine miR122, miR103, miR185, and let-7g expression levels, cDNA was first synthesized from RNA, and quantitative PCR was then performed using Mir-X miRNA First-Strand Synthesis and SYBR qRT-PCR Kit (Clontech). The expression levels of miRNA precursor were determined according to the previous report[37] using the reported primers. Relative expression values were calculated by the *CT*-based calibrated standard curve method. These calculated values were then normalized to the expression of U6 snRNA. The reverse primer was provided in the kit.

**Determining TRBP phosphorylation status.** Plasmids expressing wild-type TRBP and kinase-dead TRBP (TRBP SΔA) were kindly provided by Professor Liu[15]. Twenty-four hours after transfection into Huh7 cells with corresponding plasmids, substances were treated for 24 h, and cell lysates were collected for subsequent Western blotting. To better discriminate the phosphorylated form of TRBP from the unphosphorylated form, a Mn2+-Phos-tag SDS-PAGE gel (Wako) was used according to the manufacturer's instructions.

**Generation of miR103-expressing transgenic mice.** To construct transgenic mice, plasmids expressing miRNA-103 precursors were modified as follows: to add the SV40 poly(A) tail signal downstream of the miR103 precursor sequences, the pCDH-miR103 precursor-expressing plasmid was digested at the *Not*I restriction site, and PCR-amplified poly(A) tail signal sequences were digested with *Cla*I from the original plasmid as a template was inserted by the Infusion cloning system (Clontech, Mountain View, CA). A DNA fragment of 1,125 bp, containing the CMV promoter region, the 470-bp genomic region for the miR103 precursor, and a SV40 poly(A) tail signal, was resected from the constructed plasmid by digestion with *Cla*I. Stable C57BL/6 embryonic stem (ES) cell lines were generated by electroporation of the linearized transgene, and the resulting cells were injected into blastocysts by the UNITECH Company (Chiba, Japan). Genotyping was performed by PCR using DNA isolated from tail snips. Four different mouse lines were maintained and the male littermates were used in the experiments.

**Glucose test.** Blood glucose was tested using a Glucose Pilot system (Iwai Chemical, Japan). Glucose tolerance and pyruvate tolerance tests were performed by intraperitoneal injection of glucose (2 g/kg) or pyruvate (2 g/kg) after fasting overnight. Blood glucose levels were measured before injection (0 min) and at 15, 30, 60, and 120 min after injection.

**Adipocyte size.** Visceral fat tissues stained with hematoxylin and eosin were analyzed using the Image-J software. One hundred adipocytes were measured per animal to determine adipocyte size. The high-fat diet was purchased from CLEA-Japan (Tokyo, Japan).

**miRNA microarray analyses.** miRNA microarray analysis was performed using miRNA oligo chips (Toray Industries, Tokyo, Japan). Normalization was performed using the intensities from U6, instead of the standard global normalization. The data and the protocols were deposited in a public database (Please refer the following link during the review process; http://www.ncbi.nlm.nih.gov/geo/query/acc.cgi?token=frwpxomkicoicte&acc=GSE46526).

**Statistical analysis.** Statistically significant differences between groups were determined using Student's *t*-test when variances were equal. When variances were unequal, Welch's *t*-test was used. *P*-values less than 0.05 were considered to indicate statistical significance.


1. Surh, Y. J. Cancer chemoprevention with dietary phytochemicals. *Nat Rev Cancer* **3**, 768–780 (2003).
2. D'Incalci, M., Steward, W. P. & Gescher, A. J. Use of cancer chemopreventive phytochemicals as antineoplastic agents. *Lancet Oncol* **6**, 899–904 (2005).
3. Baur, J. A. *et al.* Resveratrol improves health and survival of mice on a high-calorie diet. *Nature* **444**, 337–342 (2006).
4. Carrington, J. & Ambros, V. Role of microRNAs in plant and animal development. *Science* **301**, 336–338 (2003).
5. Bartel, D. P. MicroRNAs: genomics, biogenesis, mechanism, and function. *Cell* **116**, 281–297 (2004).
6. Ambros, V. The functions of animal microRNAs. *Nature* **431**, 350–355 (2004).

7. Lu, J. *et al.* MicroRNA expression profiles classify human cancers. *Nature* **435**, 834–838 (2005).
8. Kojima, K. *et al.* MicroRNA122 is a key regulator of α-fetoprotein expression and influences the aggressiveness of hepatocellular carcinoma. *Nat Commun* **2**, 338 (2011).
9. Takata, A. *et al.* MicroRNA-140 acts as a liver tumor suppressor by controlling NF-κB activity by directly targeting DNA methyltransferase 1 (Dnmt1) expression. *Hepatology* **57**, 162–170 (2013).
10. Trajkovski, M. *et al.* MicroRNAs 103 and 107 regulate insulin sensitivity. *Nature* **474**, 649–653 (2011).
11. Krützfeldt, J. *et al.* Silencing of microRNAs in vivo with 'antagomirs'. *Nature* **438**, 685–689 (2005).
12. Budhraja, A. *et al.* Apigenin induces apoptosis in human leukemia cells and exhibits anti-leukemic activity in vivo. *Mol Cancer Ther* **11**, 132–142 (2012).
13. Shukla, S. *et al.* Blockade of beta-catenin signaling by plant flavonoid apigenin suppresses prostate carcinogenesis in TRAMP mice. *Cancer Res* **67**, 6925–6935 (2007).
14. Wang, W. *et al.* Cell-cycle arrest at G2/M and growth inhibition by apigenin in human colon carcinoma cell lines. *Mol Carcinog* **28**, 102–110 (2000).
15. Paroo, Z., Ye, X., Chen, S. & Liu, Q. Phosphorylation of the human microRNA-generating complex mediates MAPK/Erk signaling. *Cell* **139**, 112–122 (2009).
16. Yi Lau, G. T. & Leung, L. K. The dietary flavonoid apigenin blocks phorbol 12-myristate 13-acetate-induced COX-2 transcriptional activity in breast cell lines. *Food Chem Toxicol* **48**, 3022–3027 (2010).
17. Tatsuta, A. *et al.* Suppression by apigenin of peritoneal metastasis of intestinal adenocarcinomas induced by azoxymethane in Wistar rats. *Clin Exp Metastasis* **18**, 657–662 (2000).
18. Yin, F., Giuliano, A. E. & Van Herle, A. J. Signal pathways involved in apigenin inhibition of growth and induction of apoptosis of human anaplastic thyroid cancer cells (ARO). *Anticancer Res* **19**, 4297–4303 (1999).
19. Kuo, M. L. & Yang, N. C. Reversion of v-H-ras-transformed NIH 3T3 cells by apigenin through inhibiting mitogen activated protein kinase and its downstream oncogenes. *Biochem Biophys Res Commun* **212**, 767–775 (1995).
20. Yao, S. L. *et al.* Selective radiosensitization of p53-deficient cells by caffeine-mediated activation of p34cdc2 kinase. *Nat Med* **2**, 1140–1143 (1996).
21. Chan, L. P. *et al.* Apigenin induces apoptosis via tumor necrosis factor receptor- and Bcl-2-mediated pathway and enhances susceptibility of head and neck squamous cell carcinoma to 5-fluorouracil and cisplatin. *Biochim Biophys Acta* **1820**, 1081–1091 (2012).
22. Mafuvadze, B., Liang, Y., Besch-Williford, C., Zhang, X. & Hyder, S. M. Apigenin induces apoptosis and blocks growth of medroxyprogesterone acetate-dependent BT-474 xenograft tumors. *Horm Cancer* **3**, 160–171 (2012).
23. Nicholas, C. *et al.* Apigenin blocks lipopolysaccharide-induced lethality in vivo and proinflammatory cytokines expression by inactivating NF-kappaB through the suppression of p65 phosphorylation. *J Immunol* **179**, 7121–7127 (2007).
24. Landolfi, R., Mower, R. L. & Steiner, M. Modification of platelet function and arachidonic acid metabolism by bioflavonoids. Structure-activity relations. *Biochem Pharmacol* **33**, 1525–1530 (1984).
25. Hsu, S. H. *et al.* Essential metabolic, anti-inflammatory, and anti-tumorigenic functions of miR-122 in liver. *J Clin Invest* **122**, 2871–2883 (2012).
26. Lanford, R. E. *et al.* Therapeutic silencing of microRNA-122 in primates with chronic hepatitis C virus infection. *Science* **327**, 198–201 (2010).
27. Elmén, J. *et al.* LNA-mediated microRNA silencing in non-human primates. *Nature* **452**, 896–899 (2008).
28. Esau, C. *et al.* miR-122 regulation of lipid metabolism revealed by in vivo antisense targeting. *Cell Metab* **3**, 87–98 (2006).
29. Jopling, C. L., Yi, M., Lancaster, A. M., Lemon, S. M. & Sarnow, P. Modulation of hepatitis C virus RNA abundance by a liver-specific MicroRNA. *Science* **309**, 1577–1581 (2005).
30. Lindow, M. & Kauppinen, S. Discovering the first microRNA-targeted drug. *J Cell Biol* **199**, 407–412 (2012).
31. Ku, B. M. *et al.* Caffeine inhibits cell proliferation and regulates PKA/GSK3β pathways in U87MG human glioma cells. *Mol Cells* **31**, 275–279 (2011).
32. Nishizuka, T. *et al. Procya* nidins are potent inhibitors of LOX-1: a new player in the French Paradox. *Proc Jpn Acad Ser B Phys Biol Sci* **87**, 104–113 (2011).
33. Teraoka, M. *et al.* Cytoprotective effect of chlorogenic acid against α-synuclein-related toxicity in catecholaminergic PC12 cells. *J Clin Biochem Nutr* **51**, 122–127 (2012).
34. Shukla, S. & Gupta, S. Apigenin: a promising molecule for cancer prevention. *Pharm Res* **27**, 962–978 (2010).
35. Takata, A. *et al.* MicroRNA-22 and microRNA-140 suppress NF-κB activity by regulating the expression of NF-κB coactivators. *Biochem Biophys Res Commun* **411**, 826–831 (2011).
36. Kubota, Y., O'Grady, P., Saito, H. & Takekawa, M. Oncogenic Ras abrogates MEK SUMOylation that suppresses the ERK pathway and cell transformation. *Nat Cell Biol* **13**, 282–291 (2011).
37. Suzuki, H. I. *et al. Modulat* ion of microRNA processing by p53. *Nature* **460**, 529–533 (2009).


## Acknowledgments

This work was supported by Grants-in-Aid from the Ministry of Education, Culture, Sports, Science and Technology, Japan (#25293076 and #24390183) (to M. Otsuka and K. Koike), by Health Sciences Research Grants of The Ministry of Health, Labor and Welfare of Japan (to K. Koike), and grants from the Nestlé Nutrition Council, Japan (to A.T.), and the Foundation of All Japan Coffee Association (to M. Otsuka).

## Author contributions

M.Ohno, C.S. and M.Otsuka planned the research and wrote the paper. M.Ohno, C.S., T.K., T.Y., A.T., K.Kojima, and M.Otsuka performed the majority of the experiments. M.A. and H.Y. contributed materials. Y.K. supported several experiments. K.Koike supervised the entire project.

## Additional information

**Supplementary information** accompanies this paper at http://www.nature.com/scientificreports

**Competing financial interests:** The authors declare no competing financial interests.

**How to cite this article:** Ohno, M. *et al.* The flavonoid apigenin improves glucose tolerance through inhibition of microRNA maturation in miRNA103 transgenic mice. *Sci. Rep.* **3**, 2553; DOI:10.1038/srep02553 (2013).

EASL EUROPEAN ASSOCIATION FOR THE STUDY OF THE LIVER | JOURNAL OF HEPATOLOGY



# A genome-wide association study of HCV-induced liver cirrhosis in the Japanese population identifies novel susceptibility loci at the MHC region

Yuji Urabe[1,2], Hidenori Ochi[2], Naoya Kato[4], Vinod Kumar[1,3], Atsushi Takahashi[3], Ryosuke Muroyama[4], Naoya Hosono[3], Motoyuki Otsuka[5], Ryosuke Tateishi[5], Paulisally Hau Yi Lo[1], Chizu Tanikawa[1], Masao Omata[5], Kazuhiko Koike[5], Daiki Miki[2], Hiromi Abe[2], Naoyuki Kamatani[3], Joji Toyota[6], Hiromitsu Kumada[7], Michiaki Kubo[3], Kazuaki Chayama[2], Yusuke Nakamura[1,3], Koichi Matsuda[1,*]

[1]*Laboratory of Molecular Medicine, Human Genome Center, Institute of Medical Science, The University of Tokyo, Tokyo, Japan;* [2]*Department of Medical and Molecular Science, Division of Frontier Medical Science, Programs for Biomedical Research, Graduate School of Biomedical Sciences, Hiroshima University, Hiroshima, Japan;* [3]*Center for Genomic Medicine, The Institute of Physical and Chemical Research (RIKEN), Kanagawa, Japan;* [4]*Unit of Disease Control Genome Medicine, The Institute of Medical Science, The University of Tokyo, Tokyo, Japan;* [5]*Department of Gastroenterology, Graduate School of Medicine, The University of Tokyo, Tokyo, Japan;* [6]*Department of Gastroenterology, Sapporo Kosei General Hospital, Hokkaido, Japan;* [7]*Department of Hepatology, Toranomon Hospital, Tokyo, Japan*

**Background & Aims**: We performed a genome-wide association study (GWAS) of hepatitis C virus (HCV)-induced liver cirrhosis (LC) to identify predictive biomarkers for the risk of LC in patients with chronic hepatitis C (CHC).

**Methods**: A total of 682 HCV-induced LC cases and 1045 CHC patients of Japanese origin were genotyped by Illumina Human Hap 610-Quad bead Chip.

**Results**: Eight SNPs which showed possible associations ($p < 1.0 \times 10^{-5}$) at the GWAS stage were further genotyped using 936 LC cases and 3809 CHC patients. We found that two SNPs within the major histocompatibility complex (MHC) region on chromosome 6p21, rs910049 and rs3135363, were significantly associated with the progression from CHC to LC ($p_{combined} = 9.15 \times 10^{-11}$ and $1.45 \times 10^{-10}$, odds ratio (OR) = 1.46 and 1.37, respectively). We also found that *HLA-DQA1*0601* and *HLA-DRB1*0405* were associated with the progression from CHC to LC ($p = 4.53 \times 10^{-4}$ and $1.54 \times 10^{-4}$ with OR = 2.80 and 1.45, respectively). Multiple logistic regression analysis revealed that rs3135363, rs910049, and *HLA-DQA1*0601* were independently associated with the risk of HCV-induced LC. In addition, individuals with four or more risk alleles for these three loci have a 2.83-fold higher risk for LC than those with no risk allele, indicating the cumulative effects of these variations.

**Conclusions**: Our findings elucidated the crucial roles of multiple genetic variations within the MHC region as prognostic/predictive biomarkers for CHC patients.



## Introduction

Two million people in Japan and 210 million people worldwide are estimated to be infected with the hepatitis C virus (HCV), which is known to be a major cause of chronic viral liver disease [1]. Patients with chronic hepatitis C (CHC) usually exhibit mild inflammatory symptoms, but are at a significantly high risk for developing liver cirrhosis (LC) and hepatocellular carcinoma [2]. More than 400,000 people at present suffer from LC, which is ranked as the 9th major cause of death in Japan. In addition, liver cancer causes approximately 32,000 deaths per year, making it the 4th most common cause of death from malignant diseases. Thus, HCV-related diseases are important public health problems [3].

Clinical outcomes after the exposure to HCV vary enormously among individuals. Approximately 70% of infected persons will develop chronic hepatitis [4], and about 20–30% of CHC patients will develop cirrhosis, but others can remain asymptomatic for decades [2]. The annual death rate of patients with decompensated cirrhosis is as high as 15–30% [5]. Moreover, more than 7% of LC patients develop hepatocellular cancer in Japan and Taiwan, while the frequencies are less than 1.6% among other ethnic groups [6,7]. These inter-individual and inter-ethnic differences have been attributed to various factors such as viral genotypes,

Keywords: Genome-wide association study; Hepatitis C virus; Liver cirrhosis; Major histocompatibility complex.
*Received 22 April 2012; received in revised form 15 December 2012; accepted 24 December 2012; available online 12 January 2013*

* Corresponding author. Address: Laboratory of Molecular Medicine, Institute of Medical Science, The University of Tokyo, 4-6-1 Shirokanedai, Minato, Tokyo 108-8639, Japan. Tel.: +81 3 5449 5376; fax: +81 3 5449 5123.
*E-mail address:* koichima@ims.u-tokyo.ac.jp (K. Matsuda).

*Abbreviations:* CHC, chronic hepatitis C; GWAS, genome-wide association study; HCV, hepatitis C virus; LC, liver cirrhosis; MHC, major histocompatibility complex; OR, odds ratio; PBC, primary biliary cirrhosis; SNPs, single nucleotide polymorphisms.

**Table 1. Characteristics of samples and methods used in this study.**

| Stage | Source | Platform | Number of samples | Female (%) | Age, yr (mean ± SD) |
|---|---|---|---|---|---|
| **GWAS** | | | | | |
| Liver cirrhosis | BioBank Japan | Illumina Human Hap 610 | 682 | 313 (46.3) | 67.1 ± 9.7 |
| Chronic hepatitis C[a] | Hiroshima University | Illumina Human Hap 610 | 1045 | 371 (35.5) | 55.2 ± 11.0 |
| **Replication** | | | | | |
| Liver cirrhosis | Tokyo University | Invader assay | 716 | 334 (46.8) | 64.4 ± 10.4 |
| | Hiroshima University | | 220 | 98 (44.5) | 64.7 ± 8.98 |
| Chronic hepatitis C[a] | BioBank Japan | Invader assay | 1670 | 780 (46.8) | 59.7 ± 12.6 |
| | Hiroshima University | | 2139 | 1061 (51.8) | 58.8 ± 9.20 |

[a]Number of samples that qualified. CHC patients with severe liver fibrosis (F3 or F4) or lower platelet counts (<160,000) were excluded.

alcohol consumption, age at infection, co-infection of HIV or HBV [8–10], insulin resistance, steatosis, and metabolic syndrome [11]. Previous gene expression analyses also identified various genes associated with liver fibrosis among patients with CHC [12–14]. In addition, miRNAs such as mir-21 and mir-122 were shown to be correlated with live fibrosis [15,16].

Currently, the genome-wide association study is the most common method to identify genetic variations associated with disease risk [17–20]. In addition, the roles of genetic factors in HCV-related diseases have been elucidated. *IL28B* is associated with spontaneous clearance of HCV [21] as well as with the clinical response to the combination therapy of pegylated interferon and ribavirin [22,23]. Recently, our group has shown that SNP rs2596542 on *MICA* [24] and SNP rs1012068 on *DEPDC5* [25] are significantly associated with HCV-induced liver cancer. Although liver cirrhosis is the major risk factor of liver cancer, a fraction of CHC patients will develop HCC without accompanying LC. Therefore, the underlying genetic background would be different between HCV-induced LC and HCV-induced HCC. Previous studies identified the association of genetic variants in *HLA-DQ/DR/B* [26–28], *2-5AS* [29], *TLR3* [30], and *PNPLA3* [31] with the risk of liver fibrosis among patients with CHC. However, a comprehensive approach for HCV-induced LC has not been conducted so far. Here we performed GWAS of HCV-induced LC to identify predictive biomarkers for the risk of LC in patients with CHC.

## Materials and methods

*Ethics statement*

All subjects provided written informed consent. This project was approved by the ethical committees at University of Tokyo, Hiroshima University, Sapporo Kosei General Hospital, Toranomon Hospital, and Center for Genomic Medicine, Institutes of Physical and Chemical Research (RIKEN).

*Study population*

The characteristics of each cohort are shown in Table 1. In this study, we conducted GWAS and replication analysis on a total of 1618 HCV-induced LC and 4854 CHC patients. All subjects had abnormal levels of serum alanine transaminase for more than 6 months and were positive for both HCV antibody and serum HCV RNA. Among 1618 LC and 4854 CHC samples, 342 LC patients (21.14%) and 2997 CHC patients (61.70%) underwent liver biopsy. The remaining 1276 LC and 1857 CHC patients were diagnosed by non-invasive methods including hepatic imaging (e.g., ultrasonography, computed tomography, arteriography or magnetic resonance imaging), biochemical data (serum bilirubin, serum albumin, platelet, or prothrombin time), and the presence/absence of clinical manifestations of portal hypertension (e.g., varices, encephalopathy or ascites). The patients with CHC or LC were recruited for this study regardless of their treatment history. We excluded from the analysis the followings CHC patients: (1) advanced liver fibrosis (F3 or F4 by New Inuyama classification) [32], (2) platelet count under 160,000 for patients without liver fibrosis staging, and (3) HBV co-infection. Characteristics of each study cohort are shown in Table 1. In brief, DNA of HCV-induced LC and CHC patients was obtained from Biobank Japan (http://biobankjp.org/) [33], the Hiroshima Liver Study Group (http://home.hiroshima-u.ac.jp/naika1/researchprofile/pdf/liverstudygroupe.pdf), Toranomon Hospital, and the University of Tokyo. All subjects were of Japanese origin.

*SNP genotyping*

Genomic DNA was extracted from peripheral blood leukocytes using a standard method. In GWAS, we genotyped 682 LC and 1045 CHC samples using Illumina Human Hap 610-Quad bead Chip (Supplementary Fig. 1). Samples with low call rate (<0.98) were excluded from our analysis (six LC and two CHC samples). We then applied SNP quality control as follows: call rate $\geqslant$0.99 in LC and CHC samples, Hardy–Weinberg $p \geqslant 1 \times 10^{-6}$ in LC and CHC samples. Consequently, 461,992 SNPs on the autosomal chromosomes passed the quality control filters. SNPs with minor allele frequency of <0.01 in both LC and CHC samples were excluded from further analyses, considering statistical power in the replication analysis. Finally, we analyzed 431,618 SNPs in GWAS. Among the top ten SNPs showing $p < 1.0 \times 10^{-5}$, we selected nine SNPs for further analysis with LD threshold of $r^2 = 0.95$. In the replication stage, we genotyped 936 LC and 3809 CHC using multiplex PCR-based Invader assay (Third Wave Technologies).

*Statistical analysis*

The association of SNPs with the phenotype in the GWAS, replication stage, and combined analyses was tested by logistic regression analysis, upon adjusting for age at recruitment (continuous) and gender, by assuming additive model using PLINK [34]. In the GWAS, the genetic inflation factor $\lambda$ was derived by applying logistic regressed $p$ values for all the tested SNPs. The quantile–quantile plot was drawn using R program. The odds ratios were calculated using the non-susceptible allele as reference, unless stated otherwise. The combined analysis of GWAS and replication stage was verified by using the Mantel–Haenszel method. We set the significance threshold as follows; $p = 1 \times 10^{-5}$ in the GWAS stage (first stage) and $p = 6.25 \times 10^{-3}$ (=0.05/8) in the replication analysis. We considered $p < 5 \times 10^{-8}$ as threshold of GWAS significance in the combined analysis, which is the Bonferroni-corrected threshold for the number of independent SNPs genotyped in HapMap Phase II [35]. The heterogeneity across two stages was examined by using the Breslow–Day test [36]. We used Haploview software to analyze the association of haplotypes and LD values between SNPs. Quality control for SNPs was applied as follows: call rate $\geqslant$0.95 in LC and CHC samples, and Hardy–Weinberg $p \geqslant 1 \times 10^{-6}$ in CHC samples in replication stage. The statistical power was 19.51% in GWAS (the first stage) ($p = 1.00 \times 10^{-5}$), 97.98% in replication ($p = 0.05/8$), and 74.76% in the combined stage ($p = 5.00 \times 10^{-8}$) at minor allele frequency of 0.3 and OR of 1.3.

*Imputation-based association analysis of HLA class I and class II alleles*

We obtained an SNP or a combination of SNPs which could tag the HLA alleles in the Japanese population from a previous study [37]. Genotypes of tagging SNPs were imputed in the GWAS samples by using a Hidden Markov model programmed in MACH [38] and haplotype information from HapMap JPT samples

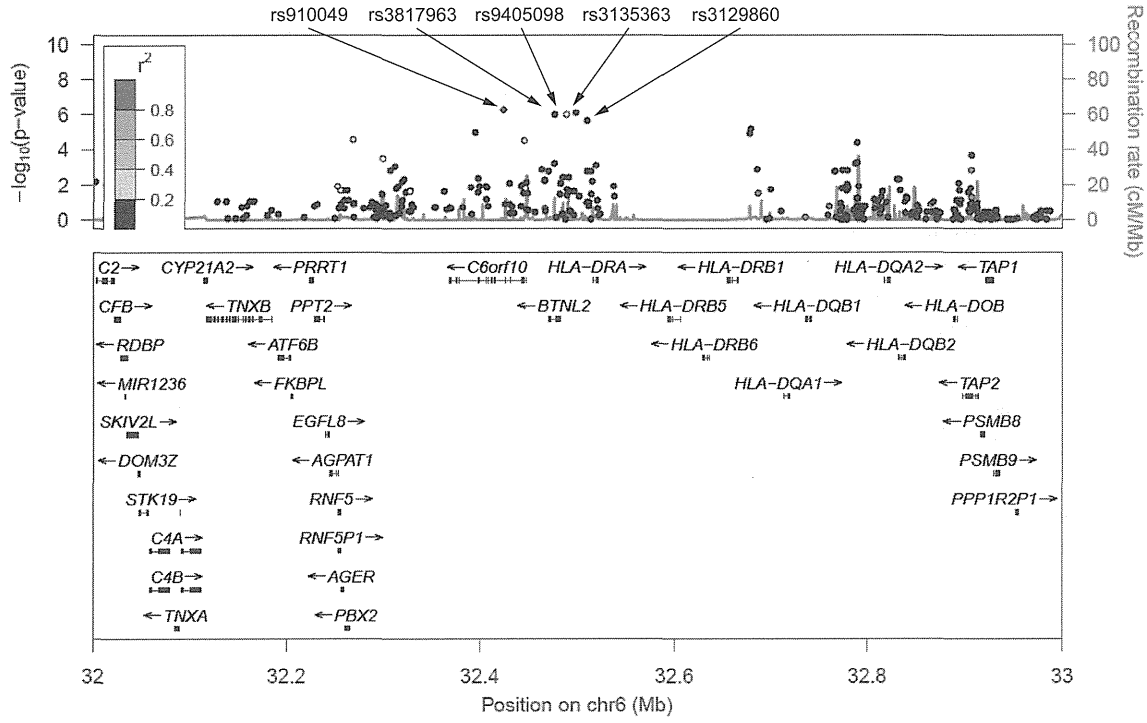


**Fig. 1. Regional association plot at 6p21.3.** (Upper panel) $p$ Values of genotyped SNPs (circle) and imputed SNPs (cross) are plotted (as $-\log_{10}$ $p$ value) against their physical position on chromosome 6 (NCBI Build 36). The $p$ value for rs910049 at GWAS is represented by a purple diamond. Estimated recombination rates from HapMap JPT show the local LD structure. Inset; the color of the other SNPs indicates LD with rs3135363 according to a scale from $r^2 = 0$ to $r^2 = 1$ based on pair-wise $r^2$ values from HapMap JPT. (Lower panel) Gene annotations from the University of California Santa Cruz genome browser.

and 1000 genome imputation samples [39]. We applied the same SNP quality criteria as in GWAS, to select SNPs for the analysis. We employed the logistic regression analysis upon age and gender adjustment to assess the associations between HCV-induced LC and HLA alleles.

*Software*

For general statistical analysis, we employed R statistical environment version 2.9.1 (cran.r-project.org) or plink-1.06 (pngu.mgh.harvard.edu/~purcell/plink/). The Haploview software version 4.2 [40] was used to calculate LD and to draw Manhattan plot. Primer3 -web v0.3.0 (http://frodo.wi.mit.edu) web tool was used to design primers. We employed LocusZoom (http://csg.sph.umich.edu/locuszoom/) for regional plots. We used SNP Functional Prediction web tool for functional annotation of SNPs (http://snpinfo.niehs.nih.gov/snpfunc.htm) [41]. We used "Gene Expression Analysis Based on Imputed Genotypes" (http://www.sph.umich.edu/csg/liang/imputation) [42] for eQTL analysis. We used MACTH [43] web tool for searching potential binding sites for transcription factors (http://www.gene-regulation.com/index.htm).

## Results

*Genome-wide association study for HCV-induced liver cirrhosis*

We performed a two-stage GWAS using a total of 1618 cases and 4854 controls (Supplementary Fig. 1). In the first stage, a whole genome scan was performed on 682 Japanese patients with HCV-induced LC and 1045 Japanese patients with CHC, using Illumina Human Hap 610-Quad bead Chip. The genotyping results of 431,618 single nucleotide polymorphisms (SNPs) obtained after our standard quality control were used for further analysis. CHC patients with severe liver fibrosis (F3 or F4 according to the New Inuyama classification [32]) or lower platelet counts (<160,000) were excluded from the control group. As progression from CHC to LC is strongly affected by age and gender, we performed logistic regression analyses including age and gender as covariates at all tested loci in our analyses. The genetic inflation factor lambda was 1.051, indicating that there is little or no evidence of population stratification (Supplementary Fig. 2A). Although no SNPs cleared the GWAS significance threshold ($p < 5 \times 10^{-8}$) at the first stage, we selected ten candidate SNPs showing suggestive association of $p < 1 \times 10^{-5}$ (Supplementary Fig. 2B and Supplementary Table 1). After excluding SNP rs6891116 due to almost absolute linkage with SNP rs10252674 ($r^2 = 0.99$), the remaining nine SNPs were further genotyped using an independent cohort, consisting of 936 LC and 3809 CHC cases, by multiplex PCR-based Invader assay as the second stage. We could successfully obtain genotype results for eight SNPs after the QC filter (call rate $\geqslant 0.95$ in LC and CHC samples, Hardy–Weinberg of $p \geqslant 1 \times 10^{-6}$ in CHC samples). The logistic regression analysis adjusted by age and gender revealed that five SNPs on chromosome 6q21.3 indicated a significant association with progression from CHC to LC after the Bonferroni correction ($p < 0.05/8 = 6.25 \times 10^{-3}$, Supplementary Table 2). A meta-analysis of the two stages with a fixed-effects model revealed that all of the five SNPs significantly associated with progression from CHC to LC ($p$ values of $9.15 \times 10^{-11}$–$1.28 \times 10^{-8}$ with odds ratios (OR) of 1.30–1.46, Fig. 1 and Table 2). These five SNPs were located in the HLA class II region and were in strong linkage disequilibrium with each other ($D'$ >0.75,

**Table 2. Summary of GWAS and replication analyses.**

| SNP | Stage | Allele (1/2) | Gene | Liver cirrhosis | | | | Chronic hepatitis C | | | | OR (95% CI)[b] | *p* value[c] | *p* value$_{het}$[d] |
|---|---|---|---|---|---|---|---|---|---|---|---|---|---|---|
| | | | | 11 | 12 | 22 | RAF[a] | 11 | 12 | 22 | RAF[a] | | | |
| rs910049 | | | | | | | | | | | | | | |
| | GWAS | a/g | *C6orf10* (6p21.3) | 24 | 217 | 435 | 0.196 | 25 | 224 | 794 | 0.131 | 1.73 (1.40-2.15) | $5.39 \times 10^{-7}$ | |
| | Replication | | | 38 | 259 | 631 | 0.180 | 66 | 952 | 2790 | 0.142 | 1.37 (1.20-1.58) | $7.59 \times 10^{-6}$ | |
| | Combined[e] | | | | | | | | | | | 1.46 (1.28-1.62) | $9.15 \times 10^{-11}$ | 0.075 |
| rs3817963 | | | | | | | | | | | | | | |
| | GWAS | a/g | *BTNL2* (6p21.3) | 92 | 343 | 241 | 0.390 | 101 | 437 | 505 | 0.306 | 1.53 (1.29-1.81) | $9.50 \times 10^{-7}$ | |
| | Replication | | | 130 | 395 | 395 | 0.356 | 409 | 1573 | 1816 | 0.315 | 1.22 (1.10-1.36) | $2.66 \times 10^{-4}$ | |
| | Combined[e] | | | | | | | | | | | 1.30 (1.18-1.42) | $1.28 \times 10^{-8}$ | 0.029 |
| rs9405098 | | | | | | | | | | | | | | |
| | GWAS | a/g | No gene (6p21.3) | 75 | 293 | 308 | 0.328 | 70 | 365 | 608 | 0.242 | 1.54 (1.30-1.84) | $1.10 \times 10^{-6}$ | |
| | Replication | | | 100 | 361 | 462 | 0.304 | 249 | 1429 | 2129 | 0.253 | 1.30 (1.16-1.46) | $5.64 \times 10^{-6}$ | |
| | Combined[e] | | | | | | | | | | | 1.37 (1.23-1.50) | $1.04 \times 10^{-10}$ | 0.105 |
| rs3135363 | | | | | | | | | | | | | | |
| | GWAS | c/t | No gene (6p21.3) | 35 | 258 | 383 | 0.757 | 89 | 447 | 507 | 0.700 | 1.58 (1.32-1.90) | $7.89 \times 10^{-7}$ | |
| | Replication | | | 73 | 322 | 540 | 0.750 | 389 | 1486 | 1929 | 0.702 | 1.30 (1.16-1.46) | $7.94 \times 10^{-6}$ | |
| | Combined[e] | | | | | | | | | | | 1.37 (1.24-1.51) | $1.45 \times 10^{-10}$ | 0.069 |
| rs3129860 | | | | | | | | | | | | | | |
| | GWAS | a/g | No gene (6p21.3) | 58 | 294 | 324 | 0.303 | 57 | 348 | 638 | 0.221 | 1.55 (1.29-1.82) | $6.45 \times 10^{-6}$ | |
| | Replication | | | 88 | 339 | 507 | 0.276 | 208 | 1341 | 2246 | 0.231 | 1.28 (1.14-1.44) | $2.53 \times 10^{-5}$ | |
| | Combined[e] | | | | | | | | | | | 1.36 (1.22-1.49) | $1.07 \times 10^{-9}$ | 0.085 |

1618 (682 in GWAS and 936 in replication) liver cirrhosis and 4854 (1045 in GWAS and 3809 in replication) chronic hepatitis C samples were analyzed.
[a]RAF, risk allele frequency.
[b]OR, odds ratios; CI, confidence interval.
[c]*p* Values obtained by logistic regression analysis adjusted for age and gender under additive model.
[d]*p* Values of heterogeneities (Phet) across three stages were examined by using the Breslow–Day test.
[e]Combined odds ratio and *p* values for independence test were calculated by Mendel-hauzen and Laird method in the meta-analysis.

Supplementary Fig. 3). To further evaluate the effect of each variation on the progression from CHC to LC, we performed multiple logistic regression analyses. As a result, rs910049 ($p$ of $1.91 \times 10^{-3}$ with OR of 1.25) and rs3135363 ($p$ of $1.49 \times 10^{-4}$ with OR of 1.23) remained significantly associated with the progression risk from CHC to LC, while the remaining three SNPs failed to show significant associations ($p > 0.05$) (Supplementary Table 3). Thus, two SNPs, rs910049 and rs3135363, seem to be independent risk factors for HCV-induced LC.

Since reduced platelet level is associated with a poor prognosis among CHC patients [44] we excluded patients with platelet level of less than 160,000 from CHC groups to increase the risk of type 2 error in this study. We also conducted the analysis using only CHC patients diagnosed with liver biopsy. As a result, both SNPs reached genome-wide significance ($p < 5 \times 10^{-8}$), although the associations were reduced due to the smaller sample size (Supplementary Table 4).

Subgroup analyses, stratified by IFN treatment status, amount of alcohol consumption, and gender, were also performed, since these factors were shown to be associated with the prognosis of CHC patients [45–47]. A total of 334 LC patients (35.83%) and 2325 CHC (82.4%) were treated with IFN therapy. Although the frequency of IFN treatment was different between CHC and LC groups, these variations associated with the LC risk regardless of IFN treatment as well as gender and alcohol consumption (Supplementary Fig. 4A–C). When we included these factors as covariates, the association of these variations with HCV-induced LC was sustained, with OR of 1.48 and 1.56, and SNP rs3135363 still reached genome-wide significance ($p = 3.95 \times 10^{-9}$) (Supplementary Table 5).

*The association of previously reported variations with HCV-induced LC*

Non-synonymous SNP rs738409 (I148M) in the *PNPLA3* gene was shown to be associated with progression of LC in the previous prospective study in Caucasians [31]. SNP rs738409 was also associated with the severity of non-alcoholic fatty liver disease in Japanese [48]. Therefore, we analyzed SNP rs738409 in our case-control cohort, but rs738409 did not significantly associate with HCV-induced LC ($p = 0.24$ and OR = 1.10), although the risk G allele was more frequent among LC than CHC (Supplementary Table 6). Our result is similar to what observed among Caucasians in the previous study, in which rs738409 increased liver cancer risk among alcoholic cirrhosis but did not among hepatitis C cirrhosis [49]. Since biological studies demonstrated that its risk allele (G) abolishes the triglyceride hydrolysis activity of *PNPLA3* [50] *PNPLA3* variation would have a strong impact on non-viral cirrhosis.

Recently, GWAS in the Caucasian population identified the association of SNPs rs4374383, rs16851720 and rs9380516 with the progression of liver fibrosis after HCV infection [51]. However, SNPs rs4374383 and rs16851720 did not exhibit significant association ($p = 0.654$ and 0.231, respectively) in our sample set. Although SNP rs9380516 exhibited the association with $p$-value of 0.015, the risk allele showed an opposite result

**Table 3. Results of three associated variations from candidate gene analyses.**

| Gene | Tagging SNP | Haplotype frequency | | OR (95% CI)[a] | | *p* value[b] |
|---|---|---|---|---|---|---|
| | | Liver cirrhosis | Chronic hepatitis C | | | |
| *DQA1*0601* | rs2736182(T) + rs2071293(A) | 0.038 | 0.019 | 2.80 | 1.38-3.32 | $4.53 \times 10^{-4}$ |
| *DRB1*0405* | rs411326(C) + rs2395185(A) + rs4599680(A) | 0.324 | 0.266 | 1.45 | 1.15-1.56 | $1.54 \times 10^{-4}$ |

Association was tested by comparing haplotype distribution between 682 liver cirrhosis and 1045 chronic hepatitis C samples in GWAS.
[a]OR, odds ratio; CI, confidence interval.
[b]*p* Values were obtained by case-control analysis of GWAS stage (*p* for haplotype were obtained by score test, implemented in R) (*DQA1*0601* and *DRB1*0405*). The *p* values obtained by logistic regression analysis adjusted for age and gender under additive model.

(Supplementary Table 6). Taken together, these SNPs would not be associated with liver fibrosis in the Japanese population.

Genes related to extracellular matrix turnover or immune response (*KRT 19*, *COL1A1*, *STMN2*, *CXCL6*, *CCR2*, *TIMP1*, *IL8*, *IL1A*, *ITGA2*, *CLDN 4*, and *IL2*) were shown to be implicated in liver fibrosis of chronic hepatitis C [14]. To further characterize these loci, we conducted imputation analyses in the GWAS sample set (682 cases and 1045 controls), using data from HAPMAP phase II (JPT), and found 163 SNPs in 9 loci. However, none of these SNPs indicated significant association with *p*-value of less than 0.01 (Supplementary Table 7). Thus, variations of these genes did not associate with progression from chronic hepatitis C to liver cirrhosis.

### *Imputation-based fine mapping of HLA region*

The most significantly associated SNP rs3135363 is located within an intergenic region between *BTNL2* and *HLA-DRA*, and rs910049 is located in intron 7 of *C6orf10* gene (Supplementary Figs. 5 and 6). To further characterize these loci, we conducted imputation-based association analysis for the GWAS samples (682 LC and 1045 CHC samples) using data from HAPMAP Phase II (JPT), and could obtain the results of nearly 6000 SNPs in a 4-Mb genomic region. The regional association plots revealed that all modestly-associated SNPs are confined within a 700-kb region containing 21 genes, namely *TNXB*, *ATF6B*, *FKBPL*, *PRRT1*, *PPT2*, *EGFL8*, *AGPAT1*, *RNF5*, *RNF5P1*, *AGER*, *PBX2*, *C6orf10*, *BTNL2*, *HLA-DRA*, *HLA-DRB5*, *HLA-DRB6*, *HLA-DRB1*, *HLA-DQA1*, *HLA-DQA2*, *HLA-DQB1* and *HLA-DQB2* (Supplementary Fig. 5). Although 640 SNPs, including ten non-synonymous SNPs within the 4-Mb region, showed very modest associations ($p < 0.01$) with HCV-induced LC, none of these SNPs in this region revealed strong association with HCV-induced LC, after adjustment with the two SNPs, rs910049 and rs3135363 (Supplementary Fig. 7). Taken together, the associations observed in this region would reflect the association with rs910049 and rs3135363.

Previous reports indicated the association of *HLA-DRB1* and *HLA-DQ* alleles with HCV-induced chronic hepatitis in the Japanese population [26]. To investigate the association of HLA alleles with HCV-induced LC, we estimated the genotypes at the HLA region by applying the imputation results of HLA-tagging SNPs [37]. We could successfully determine 53 alleles of *HLA-A*, *B*, *C*, *DQA*, *DQB*, and *DRB* genes and find that *HLA-DQA1*0601* and *HLA-DRB1*0405* were strongly associated with HCV-induced LC ($p$ values of $4.53 \times 10^{-4}$ and $1.54 \times 10^{-4}$ with ORs of 2.80 and 1.45) even after the Bonferroni correction ($p < 0.05/53 = 9.43 \times 10^{-4}$) (Table 3 and Supplementary Table 8A–E) [37].

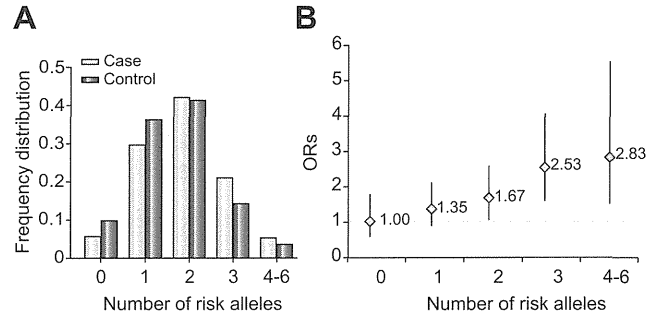


**Fig. 2. Cumulative effects of liver cirrhosis risk alleles.** (A) Frequency distribution divided by risk allele numbers (rs910049, rs3135353, and *HLA-DQA0601*) among liver cirrhosis (light blue bars) and chronic hepatitis C (dark blue bars) patients. (B) Plot of the increase odds ratio (OR) for liver cirrhosis according to the number of risk alleles. The ORs are relative to the subjects with no risk alleles (rs910049, rs3135353, and *HLA-DQA0601*). Vertical bars correspond to 95% confidence intervals. Horizontal line marks the null value (OR = 1).

### *Cumulative effect of multiple loci within the HLA region*

SNPs rs3135363 and rs910049, *HLA-DQA1*0601*, and *HLA-DRB1*0405* are located within a 300-kb segment in the HLA class II region and show moderate linkage disequilibrium (Supplementary Fig. 8). To further evaluate these genetic factors, we performed multiple logistic regression analyses and found that rs910049 ($p$ of $9.40 \times 10^{-3}$ with OR of 1.38), rs3135363 ($p$ of $3.94 \times 10^{-4}$ with OR = 1.41), and *HLA-DQA1*0601* ($p$ of $7.79 \times 10^{-3}$ with OR of 1.54) were significantly associated with HCV-induced LC (Supplementary Table 9), indicating these three variations were independent risk factors for progression of CHC to LC.

To investigate the pathophysiological roles of rs910049 and rs3135363 in disease progression, we searched the eQTL database (http://www.sph.umich.edu/csg/liang/imputation) and found that risk alleles of rs910049 (A) and rs3135363 (T) were associated with lower expression of *HLA-DQA* (LOD of $\geqslant$6.86 and 17.31, respectively) and *DRB1* (LOD of $\geqslant$12.01 and 18.96, respectively), and with higher expression of *HLA-DQB1* (LOD of $\geqslant$6.76 and 4.46, respectively) (Supplementary Table 10). Thus, rs910049 and rs3135363 are likely to affect the expression of HLA class II molecules and subsequently alter the risk of HCV-induced LC.

Finally, we examined the cumulative effects of rs910049, rs3135363, and *HLA-DQA1*0601*. Individuals with four or more risk alleles (8.8% of general population) have 2.83-fold higher risk of HCV-induced LC compared with those with no risk allele (15.0% of general population, Fig. 2).

## Discussion

We here demonstrated that multiple genetic variations in the MHC region were significantly associated with the risk of disease progression from CHC to LC, using a total of 1618 HCV-LC and 4854 CHC cases. Since a substantial proportion of patients with CHC show progression to LC in a certain time period, exclusion of CHC patients who have a high risk for LC from control subjects is essential to reduce the risk of false negative association. In this study, CHC patients with advanced fibrosis (F3 or F4 in stage) or with reduced platelet level (less than 160,000/μl) were excluded from the control samples, since these alterations are well-known risk factors for LC development [9,32]. Consequently, we were successfully able to identify the HCV-induced LC loci.

HLA genes are known to play critical roles in the regulation of our immune responses through controlling the antigen presentation to CD8 (class I) and CD4 (class II) T cells. Although previous studies indicated the association of HLA class I alleles such as *HLA-B57*, *HLA-A11*, and *HLA-C04* with persistent HCV infection [52,53], no SNPs in the HLA class I region exhibited strong association with HCV-induced LC. Here we identified three variations (rs910049, rs3135363, *HLA-DQA1*0601*) in the HLA class II region to be significantly associated with the progression risk from CHC to LC. Since two SNPs, rs910049 and rs3135363, had been indicated to affect expression levels of *HLA-DRB1* and *DQ*, our findings indicated the significant pathophysiological roles of HLA class II molecules in the development of HCV-induced liver fibrosis. Considering the function of *HLA-DQ* and *HLA-DR*, we suggest that the antigen presentation by HLA class II molecules is likely to play a critical role in the elimination of HCV-infected liver cells and subsequently prevent HCV-induced LC.

Direct acting antiviral drugs for HCV can cure up to 75% of patients infected with HCV genotype 1, and the lifetime risk of developing LC and HCC among HCV carriers was decreased during the two recent decades [54,13]. However, the amino acid sequence of the NS3 protease domain varies significantly between HCV genotypes and the antiviral efficacy differs in different HCV genotypes [55]. Moreover, protease inhibitors increased the incidence of adverse reactions such as anemia and skin rash [56]. Therefore, estimation of liver cirrhosis risk and prediction of treatment response would be essential to provide a personalized treatment and to achieve the optimal results. Due to the recent advances in pharmacogenetic studies, genetic factors associated with efficacy and adverse effects of anti-HCV treatment were identified. *IL-28B* is a powerful predictor of treatment outcome of pegylated interferon and ribavirin therapy [22], while a genetic variation in the *ITPA* gene was shown to be associated with ribavirin-induced anemia [57]. Since we conducted a retrospective study, and the majority of LC patients did not receive IFN treatment, we could not evaluate the treatment responses in our study design. However, SNPs identified in this study were associated with the LC risk independent of IFN treatment. Although the impact of each SNP was relatively weak compared with viral factors (HCV genotype, core and NS5A mutation [58]) and host factors (age, gender, obesity, and insulin resistance), we found that individuals with three or more risk alleles have a nearly three-fold higher risk of LC than those with no risk allele. Since lifetime risk of HCC development among HCV carriers is as high as about 27% for male and 8% for female [59], these three loci would have the strong effect on the clinical outcome of CHC patients. In general, the progression from chronic hepatitis C to liver cirrhosis usually takes more than 20–30 years. Therefore, a large scale prospective cohort study with more than 10-year follow-up is essential to evaluate the role of these variations as a prognostic biomarker. We would like to perform prospective analysis in future studies. We hope that our findings would contribute to clarify the underling molecular mechanism of HCV-induced liver cirrhosis.

## Financial support

This work was conducted as a part of the BioBank Japan Project that was supported by the Ministry of Education, Culture, Sports, Science and Technology of the Japanese government.

## Conflict of interest

The authors who have taken part in this study declared that they do not have anything to disclose regarding funding or conflict of interest with respect to this manuscript.

## Authors' contributions

Y. U., K. K., K. C., and K.M. conceived and designed the study; Y. U., H. O., N. K., Y. K., R. M., N. H., and M. K. performed genotyping; A. T., P. H. Y. L., C. T., and N. K. performed quality control at genome-wide phase; M. O., R. T., M. O., K. K., D. M., H. A., J. T., H. K., Y. N., K. M. and M. K. managed DNA samples; Y. U. analyzed and summarized the whole results; Y. U., Y. N., and K. M. wrote the manuscript; Y. N. obtained funding for the study.

## Acknowledgments

We thank Ayako Matsui and Hiroe Tagaya (the University of Tokyo), and the technical staff of the Laboratory for Genotyping Development, Center for Genomic Medicine, RIKEN, for their technical support.

## Supplementary data

Supplementary data associated with this article can be found, in the online version, at http://dx.doi.org/10.1016/j.jhep.2012.12.024.

## References

[1] Shepard CW, Finelli L, Alter MJ. Global epidemiology of hepatitis C virus infection. Lancet Infect Dis 2005;5:558–567.
[2] Seeff LB. Natural history of chronic hepatitis C. Hepatology 2002;36:S35–S46.
[3] Thomas DL, Seeff LB. Natural history of hepatitis C. Clin Liver Dis 2005;9:383–398, vi.
[4] Freeman AJ, Dore GJ, Law MG, Thorpe M, Von Overbeck J, Lloyd AR, et al. Estimating progression to cirrhosis in chronic hepatitis C virus infection. Hepatology 2001;34:809–816.
[5] Hoofnagle JH. Hepatitis C: the clinical spectrum of disease. Hepatology 1997;26:15S–20S.
[6] Tanaka H, Imai Y, Hiramatsu N, Ito Y, Imanaka K, Oshita M, et al. Declining incidence of hepatocellular carcinoma in Osaka, Japan, from 1990 to 2003. Ann Intern Med 2008;148:820–826.

[7] Global burden of disease (GBD) for hepatitis C. J Clin Pharmacol 2004;44:20–29.
[8] Poynard T, Bedossa P, Opolon P. Natural history of liver fibrosis progression in patients with chronic hepatitis C. The OBSVIRC, METAVIR, CLINIVIR, and DOSVIRC groups. Lancet 1997;349:825–832.
[9] Yoshida H, Shiratori Y, Moriyama M, Arakawa Y, Ide T, Sata M, et al. Interferon therapy reduces the risk for hepatocellular carcinoma: national surveillance program of cirrhotic and noncirrhotic patients with chronic hepatitis C in Japan. IHIT Study Group. Inhibition of hepatocarcinogenesis by interferon therapy. Ann Intern Med 1999;131:174–181.
[10] Zhang Q, Tanaka K, Sun P, Nakata M, Yamamoto R, Sakimura K, et al. Suppression of synaptic plasticity by cerebrospinal fluid from anti-NMDA receptor encephalitis patients. Neurobiol Dis 2012;45:610–615.
[11] Aghemo A, Prati GM, Rumi MG, Soffredini R, D'Ambrosio R, Orsi E, et al. A sustained virological response prevents development of insulin resistance in chronic hepatitis C patients. Hepatology 2012;56:549–556.
[12] Bièche I, Asselah T, Laurendeau I, Vidaud D, Degot C, Paradis V, et al. Molecular profiling of early stage liver fibrosis in patients with chronic hepatitis C virus infection. Virology 2005;332:130–144.
[13] Estrabaud E, Vidaud M, Marcellin P, Asselah T. Genomics and HCV infection: progression of fibrosis and treatment response. J Hepatol 2012;57:1110–1125.
[14] Asselah T, Bièche I, Laurendeau I, Paradis V, Vidaud D, Degott C, et al. Liver gene expression signature of mild fibrosis in patients with chronic hepatitis C. Gastroenterology 2005;129:2064–2075.
[15] Marquez RT, Bandyopadhyay S, Wendlandt EB, Keck K, Hoffer BA, Icardi MS, et al. Correlation between microRNA expression levels and clinical parameters associated with chronic hepatitis C viral infection in humans. Lab Invest 2010;90:1727–1736.
[16] Morita K, Taketomi A, Shirabe K, Umeda K, Kayashima H, Ninomiya M, et al. Clinical significance and potential of hepatic microRNA-122 expression in hepatitis C. Liver Int 2011;31:474–484.
[17] Cui R, Okada Y, Jang SG, Ku JL, Park JG, Kamatani Y, et al. Common variant in 6q26-q27 is associated with distal colon cancer in an Asian population. Gut 2011;60:799–805.
[18] Kumar V, Matsuo K, Takahashi A, Hosono N, Tsunoda T, Kamatani N, et al. Common variants on 14q32 and 13q12 are associated with DLBCL susceptibility. J Hum Genet 2011;56:436–439.
[19] Tanikawa C, Urabe Y, Matsuo K, Kubo M, Takahashi A, Ito H, et al. A genome-wide association study identifies two susceptibility loci for duodenal ulcer in the Japanese population. Nat Genet 2012;44:430–434.
[20] Urabe Y, Tanikawa C, Takahashi A, Okada Y, Morizono T, Tsunoda T, et al. A genome-wide association study of nephrolithiasis in the Japanese population identifies novel susceptible loci at 5q35.3, 7p14.3, and 13q14.1. PLoS Genet 2012;8:e1002541.
[21] Thomas DL, Thio CL, Martin MP, Qi Y, Ge D, O'Huigin C, et al. Genetic variation in *IL28B* and spontaneous clearance of hepatitis C virus. Nature 2009;461:798–801.
[22] Tanaka Y, Nishida N, Sugiyama M, Kurosaki M, Matsuura K, Sakamoto N, et al. Genome-wide association of IL28B with response to pegylated interferon-alpha and ribavirin therapy for chronic hepatitis C. Nat Genet 2009;41:1105–1109.
[23] Suppiah V, Moldovan M, Ahlenstiel G, Berg T, Weltman M, Abate ML, et al. IL28B is associated with response to chronic hepatitis C interferon-alpha and ribavirin therapy. Nat Genet 2009;41:1100–1104.
[24] Kumar V, Kato N, Urabe Y, Takahashi A, Muroyama R, Hosono N, et al. Genome-wide association study identifies a susceptibility locus for HCV-induced hepatocellular carcinoma. Nat Genet 2011;43:455–458.
[25] Miki D, Ochi H, Hayes CN, Abe H, Yoshima T, Aikata H, et al. Variation in the DEPDC5 locus is associated with progression to hepatocellular carcinoma in chronic hepatitis C virus carriers. Nat Genet 2011;43:797–800.
[26] Kuzushita N, Hayashi N, Moribe T, Katayama K, Kanto T, Nakatani S, et al. Influence of HLA haplotypes on the clinical courses of individuals infected with hepatitis C virus. Hepatology 1998;27:240–244.
[27] Singh R, Kaul R, Kaul A, Khan K. A comparative review of HLA associations with hepatitis B and C viral infections across global populations. World J Gastroenterol 2007;13:1770–1787.
[28] Mosaad YM, Farag RE, Arafa MM, Eletreby S, El-Alfy HA, Eldeek BS, et al. Association of human leucocyte antigen Class I (HLA-A and HLA-B) with chronic hepatitis C virus infection in Egyptian patients. Scand J Immunol 2010;72:548–553.
[29] Li CZ, Kato N, Chang JH, Muroyama R, Shao RX, Dharel N, et al. Polymorphism of OAS-1 determines liver fibrosis progression in hepatitis C by reduced ability to inhibit viral replication. Liver Int 2009;29:1413–1421.
[30] Mozer-Lisewska I, Sikora J, Kowala-Piaskowska A, Kaczmarek M, Dworacki G, Zeromski J. The incidence and significance of pattern-recognition receptors in chronic viral hepatitis types B and C in man. Arch Immunol Ther Exp (Warsz) 2010;58:295–302.
[31] Trépo E, Pradat P, Potthoff A, Momozawa Y, Quertinmont E, Gustot T, et al. Impact of patatin-like phospholipase-3 (rs738409 C>G) polymorphism on fibrosis progression and steatosis in chronic hepatitis C. Hepatology 2011;54:60–69.
[32] Romero-Gómez M, Gómez-González E, Madrazo A, Vera-Valencia M, Rodrigo L, Pérez-Alvarez R, et al. Optical analysis of computed tomography images of the liver predicts fibrosis stage and distribution in chronic hepatitis C. Hepatology 2008;47:810–816.
[33] Nakamura Y. The BioBank Japan project. Clin Adv Hematol Oncol 2007;5:696–697.
[34] Purcell S, Neale B, Todd-Brown K, Thomas L, Ferreira M, Bender D, et al. PLINK: a tool set for whole-genome association and population-based linkage analyses. Am J Hum Genet 2007;81:559–575.
[35] Frazer KA, Ballinger DG, Cox DR, Hinds DA, Stuve LL, Gibbs RA, et al. A second generation human haplotype map of over 3.1 million SNPs. Nature 2007;449:851–861.
[36] Breslow NE, Day NE. Statistical methods in cancer research. The design and analysis of cohort studies. IARC Sci Publ 1987;II:1–406.
[37] de Bakker PI, McVean G, Sabeti PC, Miretti MM, Green T, Marchini J, et al. A high-resolution HLA and SNP haplotype map for disease association studies in the extended human MHC. Nat Genet 2006;38:1166–1172.
[38] Scott LJ, Mohlke KL, Bonnycastle LL, Willer CJ, Li Y, Duren WL, et al. A genome-wide association study of type 2 diabetes in Finns detects multiple susceptibility variants. Science 2007;316:1341–1345.
[39] Consortium GP. A map of human genome variation from population-scale sequencing. Nature 2010;467:1061–1073.
[40] Barrett J, Fry B, Maller J, Daly M. Haploview: analysis and visualization of LD and haplotype maps. Bioinformatics 2005;21:263–265.
[41] Xu Z, Taylor JA. SNPinfo: integrating GWAS and candidate gene information into functional SNP selection for genetic association studies. Nucleic Acids Res 2009;37:W600–W605.
[42] Dixon AL, Liang L, Moffatt MF, Chen W, Heath S, Wong KC, et al. A genome-wide association study of global gene expression. Nat Genet 2007;39:1202–1207.
[43] Kel AE, Gössling E, Reuter I, Cheremushkin E, Kel-Margoulis OV, Wingender E. MATCH: a tool for searching transcription factor binding sites in DNA sequences. Nucleic Acids Res 2003;31:3576–3579.
[44] Wai CT, Greenson JK, Fontana RJ, Kalbfleisch JD, Marrero JA, Conjeevaram HS, et al. A simple noninvasive index can predict both significant fibrosis and cirrhosis in patients with chronic hepatitis C. Hepatology 2003;38:518–526.
[45] Cammà C, Di Bona D, Schepis F, Heathcote EJ, Zeuzem S, Pockros PJ, et al. Effect of peginterferon alfa-2a on liver histology in chronic hepatitis C: a meta-analysis of individual patient data. Hepatology 2004;39:333–342.
[46] Marcellin P, Asselah T, Boyer N. Fibrosis and disease progression in hepatitis C. Hepatology 2002;36:S47–S56.
[47] Silini E, Bottelli R, Asti M, Bruno S, Candusso ME, Brambilla S, et al. Hepatitis C virus genotypes and risk of hepatocellular carcinoma in cirrhosis: a case-control study. Gastroenterology 1996;111:199–205.
[48] Kawaguchi T, Sumida Y, Umemura A, Matsuo K, Takahashi M, Takamura T, et al. Genetic polymorphisms of the human PNPLA3 gene are strongly associated with severity of non-alcoholic fatty liver disease in japanese. PLoS One 2012;7:e38322.
[49] Nischalke HD, Berger C, Luda C, Berg T, Müller T, Grünhage F, et al. The PNPLA3 rs738409 148M/M genotype is a risk factor for liver cancer in alcoholic cirrhosis but shows no or weak association in hepatitis C cirrhosis. PLoS One 2011;6:e27087.
[50] He S, McPhaul C, Li JZ, Garuti R, Kinch L, Grishin NV, et al. A sequence variation (I148M) in PNPLA3 associated with nonalcoholic fatty liver disease disrupts triglyceride hydrolysis. J Biol Chem 2010;285:6706.
[51] Patin E, Kutalik Z, Guergnon J, Bibert S, Nalpas B, Jouanguy E, et al. Genome-wide association study identifies variants associated with progression of liver fibrosis from HCV infection. Gastroenterology 2012;143:124–152, e1–12.
[52] Kim AY, Kuntzen T, Timm J, Nolan BE, Baca MA, Reyor LL, et al. Spontaneous control of HCV is associated with expression of HLA-B 57 and preservation of targeted epitopes. Gastroenterology 2011;140:e681.
[53] Fanning LJ, Kenny-Walsh E, Shanahan F. Persistence of hepatitis C virus in a white population: associations with human leukocyte antigen class 1. Hum Immunol 2004;65:745–751.

[54] Imhof I, Simmonds P. Genotype differences in susceptibility and resistance development of hepatitis C virus to protease inhibitors telaprevir (VX-950) and danoprevir (ITMN-191). Hepatology 2011;53:1090–1099.
[55] Asselah T, Marcellin P. Direct acting antivirals for the treatment of chronic hepatitis C: one pill a day for tomorrow. Liver Int 2012;32: 88–102.
[56] Ozeki I, Akaike J, Karino Y, Arakawa T, Kuwata Y, Ohmura T, et al. Antiviral effects of peginterferon alpha-2b and ribavirin following 24-week monotherapy of telaprevir in Japanese hepatitis C patients. J Gastroenterol 2011;46:929–937.
[57] Ochi H, Maekawa T, Abe H, Hayashida Y, Nakano R, Kubo M, et al. ITPA polymorphism affects ribavirin-induced anemia and outcomes of therapy – a genome-wide study of Japanese HCV virus patients. Gastroenterology 2010;139:1190–1197.
[58] Enomoto N, Sakuma I, Asahina Y, Kurosaki M, Murakami T, Yamamoto C, et al. Mutations in the nonstructural protein 5A gene and response to interferon in patients with chronic hepatitis C virus 1b infection. N Engl J Med 1996;334:77–82.
[59] Huang YT, Jen CL, Yang HI, Lee MH, Su J, Lu SN, et al. Lifetime risk and sex difference of hepatocellular carcinoma among patients with chronic hepatitis B and C. J Clin Oncol 2011;29:3643–3650.

HEPATOLOGY
Official Journal of the American Association for the Study of Liver Diseases

# MicroRNA-140 Acts as a Liver Tumor Suppressor by Controlling NF-κB Activity by Directly Targeting DNa Methyltransferase 1 (Dnmt1) Expression

Akemi Takata,[1] Motoyuki Otsuka,[1] Takeshi Yoshikawa,[1] Takahiro Kishikawa,[1] Yohko Hikiba,[2] Shuntaro Obi,[3] Tadashi Goto,[1] Young Jun Kang,[4] Shin Maeda,[1] Haruhiko Yoshida,[1] Masao Omata,[1] Hiroshi Asahara,[5,6,7] and Kazuhiko Koike[1]

**MicroRNAs (miRNAs) are small RNAs that regulate the expression of specific target genes. While deregulated miRNA expression levels have been detected in many tumors, whether miRNA functional impairment is also involved in carcinogenesis remains unknown. We investigated whether deregulation of miRNA machinery components and subsequent functional impairment of miRNAs are involved in hepatocarcinogenesis. Among miRNA-containing ribonucleoprotein complex components, reduced expression of DDX20 was frequently observed in human hepatocellular carcinomas, in which enhanced nuclear factor-κB (NF-κB) activity is believed to be closely linked to carcinogenesis. Because DDX20 normally suppresses NF-κB activity by preferentially regulating the function of the NF-κB-suppressing miRNA-140, we hypothesized that impairment of miRNA-140 function may be involved in hepatocarcinogenesis. DNA methyltransferase 1 (Dnmt1) was identified as a direct target of miRNA-140, and increased Dnmt1 expression in DDX20-deficient cells hypermethylated the promoters of metallothionein genes, resulting in decreased metallothionein expression leading to enhanced NF-κB activity. MiRNA-140-knockout mice were prone to hepatocarcinogenesis and had a phenotype similar to that of DDX20 deficiency, suggesting that miRNA-140 plays a central role in DDX20 deficiency-related pathogenesis. *Conclusion*: These results indicate that miRNA-140 acts as a liver tumor suppressor, and that impairment of miRNA-140 function due to a deficiency of DDX20, a miRNA machinery component, could lead to hepatocarcinogenesis.** (HEPATOLOGY 2013;57:162-170)

Hepatocellular carcinoma (HCC) is the third most common cause of cancer-related mortality worldwide.[1] Although multiple major risk factors have been identified, such as infection with hepatitis viruses B or C, the molecular mechanisms underlying HCC development remain poorly understood, hindering the development of novel therapeutic approaches. Therefore, a better understanding of the molecular pathways involved in hepatocarcinogenesis is critical for the development of new therapeutic options.

Nuclear factor-κB (NF-κB) is one of the best-characterized intracellular signaling pathways. Its activation is a common feature of human HCC.[2-4] It acts as an inhibitor of apoptosis and as a tumor promoter[4,5] and is associated with the acquisition of a transformed phenotype during hepatocarcinogenesis.[6] In fact, studies using patient samples suggest that NF-κB activation in the liver leads to the development of HCC.[7] Although there are conflicting reports,[8] activation of the NF-κB pathway in the liver is crucial for the initiation and promotion of HCC.[4]

*Abbreviations: DEN, diethylnitrosamine; Dnmt1, DNA methyltransferase 1; HCC, hepatocellular carcinoma; miRNA; microRNA; miRNP, miRNA-containing ribonucleoprotein; MT, metallothionein; NF-κB, nuclear factor-κB; RT-PCR, reverse-transcription polymerase chain reaction; TNF-α, tumor necrosis factor-α; TRAIL, TNF-related apoptosis-inducing ligand; UTR, untranslated region.*

*From the [1]Department of Gastroenterology, Graduate School of Medicine, The University of Tokyo, Tokyo, Japan; the [2]Division of Gastroenterology, Institute for Adult Diseases, Asahi Life Foundation, Tokyo, Japan; the [3]Department of Hepatology, Kyoundo Hospital, Tokyo, Japan; the [4]Department of Immunology and Microbial Science, and the [5]Department of Molecular and Experimental Medicine, The Scripps Research Institute, La Jolla, CA; the [6]Department of Systems BioMedicine, Tokyo Medical and Dental University, Tokyo, Japan; and [7]CREST, Japan Science and Technology Agency, Tokyo, Japan.*

*Received March 30, 2012; accepted July 18, 2012.*

*Supported by Grants-in-Aid from the Ministry of Education, Culture, Sports, Science and Technology, Japan (#22390058, #23590960, and #20390204) (M. O., T. G., and K. K.); Health Sciences Research Grants from the Ministry of Health, Labor and Welfare of Japan (Research on Hepatitis) (to K. K.); National Institutes of Health Grant R01AI088229 (to Y. J. K.); the Miyakawa Memorial Research Foundation (to A. T.); and grants from the Sagawa Foundation for Promotion of Cancer Research, the Astellas Foundation for Research on Metabolic Disorders, and the Cell Science Research Foundation (to M. O.).*

MicroRNAs (miRNAs) are small RNA molecules that regulate the expression of target genes and are involved in various biological functions.[9-12] Although specific miRNAs can function as either suppressors or oncogenes in tumor development, a general reduction in miRNA expression is commonly observed in human cancers.[13-22] In this context, it can be hypothesized that deregulation of the machinery components involved in miRNA function may be related to the functional impairment of miRNAs and the pathogenesis of carcinogenesis.

In this study, we show that the expression of DDX20, an miRNA-containing ribonucleoprotein (miRNP) component, is frequently decreased in human HCC. Because DDX20 is required for both the preferential loading of miRNA-140 into the RNA-induced silencing complex and its function,[23] we hypothesized that DDX20 deficiency would lead to hepatocarcinogenesis via impaired miRNA-140 function. MiRNA-140 knockout mice were indeed more prone to hepatocarcinogenesis, and we identified a possible molecular pathway from DDX20 deficiency to liver cancer.

## Materials and Methods

***Mouse and Liver Tumor Induction.*** MiRNA-140$^{-/-}$ mice have been described.[24] Recombinant murine tumor necrosis factor-α (TNF-α) (25 μg/kg; Wako, Osaka, Japan) was injected into the tail vein, and the mice were sacrificed 1 hour later. To induce liver tumors, 15-day-old mice received an intraperitoneal injection of diethylnitrosamine (DEN) (25 mg/kg body weight), and were sacrificed 32 weeks later. All animal experiments were performed in compliance with the regulations of the Animal Use Committee of the University of Tokyo and the Institute for Adult Disease, Asahi Life Foundation.

***Plasmids.*** FLAG-tagged human DDX20-expressing plasmids were as described.[23] The pGL3-based reporter plasmid containing Dnmt1 3′ untranslated region (UTR) sequences was provided by G. Marucucci.[25]

***Detailed Materials and Methods.*** The detailed experimental procedures of clinical samples, cells, plasmids, reporter assays, reverse-transcription polymerase chain reaction (RT-PCR) analysis, antibodies, western blotting, cell assays, immunohistochemistry, microarray analysis, methylation analysis, and electrophoretic mobility-shift assay are described in the Supporting Information.

***Statistical Analysis.*** Statistically significant differences between groups were determined using a Wilcoxon rank-sum test. A Wilcoxon signed-rank test was used for statistical comparisons of protein expression levels between HCC and surrounding noncancerous tissues.

**Table 1. Cases with Differential Expression Levels of miRNP Components in HCC (n = 10)**

| Gene ID | Gene Symbol | Decreased | Increased | No Change |
|---|---|---|---|---|
| 23405 | Dicer1 | 2 | 1 | 7 |
| 27161 | EIF2C2 (AGO2) | 1 | 1 | 8 |
| 6895 | TARBP2(TRBP2) | 2 | 0 | 8 |
| 11218 | DDX20 (GEMIN3) | 8 | 0 | 2 |
| 50628 | GEMIN4 | 1 | 0 | 9 |

The expression levels of each miRNP component were determined via immunohistochemistry.

The numbers indicate the number of cases that had the differential expression levels (decreased, increased, or no change) in HCC tissues compared with those in surrounding liver tissues.

## Results

***DDX20 Expression Is Frequently Decreased in HCC.*** The expression levels of proteins reported to be miRNP components (Dicer, Ago2, TRBP2, DDX20 [also known as Gemin3], and Gemin4)[26] were initially determined via immunohistochemistry in HCC and noncancerous background liver tissues from 10 patients. DDX20 expression was lower in HCC tissue compared with the surrounding noncancerous tissue in 8 of 10 cases, whereas expression of the other genes was unchanged (Table 1 and Supporting Fig. 1). Therefore, and because DDX20 was recently identified as a possible liver tumor suppressor in mice,[27] we determined its role as a human HCC suppressor.

DDX20 protein expression was lower in several HCC cell lines, such as Huh7 and Hep3B (Fig. 1A), compared with normal hepatocytes. DDX20 protein levels were also lower in human HCC needle biopsy specimens than in surrounding noncancerous liver tissue (Fig. 1B). Immunohistochemical analysis

*Address reprint requests to: Motoyuki Otsuka, M.D., Department of Gastroenterology, Graduate School of Medicine, University of Tokyo, 7-3-1 Hongo, Bunkyo-ku, Tokyo 113-8655, Japan. E-mail: otsukamo-tky@umin.ac.jp; fax: (81)-3-3814-0021.*



*View this article online at wileyonlinelibrary.com.*

*DOI 10.1002/hep.26011*

*Potential conflict of interest: Nothing to report.*

*Additional Supporting Information may be found in the online version of this article.*

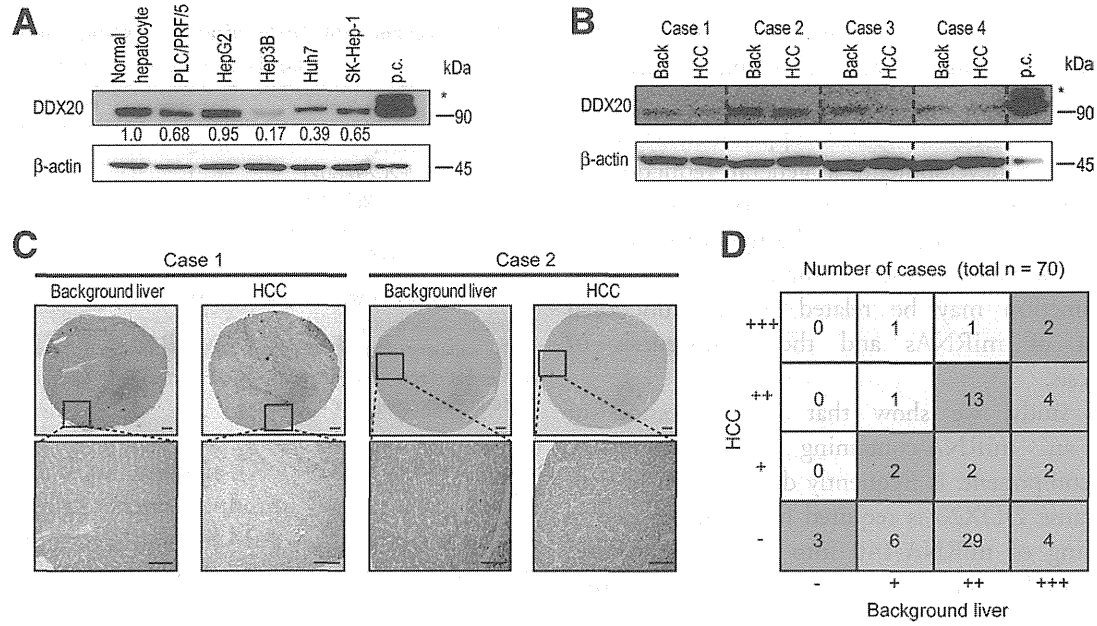


Fig. 1. Reduced DDX20 expression levels in hepatocellular carcinoma. (A) DDX20 protein expression in HCC cell lines. Numbers between the panels indicate DDX20 protein levels normalized to $\beta$-actin levels. Lysates of 293T cells transiently transfected with a FLAG-tagged DDX20-expressing plasmid yielded two DDX20 bands corresponding to the endogenous DDX20 protein and the transfected FLAG-tagged DDX20 protein (*) as a positive control (p.c.; far right lane). Data represent the results of three independent determinations. (B) DDX20 protein expression in four HCC needle biopsy specimens and in the surrounding noncancerous background liver tissue (Back). *Positive control. (C) Immunohistochemical analysis of DDX20 protein expression in HCC and surrounding tissues (background liver). Two representative cases are shown. Scale bars, 500 $\mu$m. The lower panels display magnified images of the boxed areas in the upper panels. (D) Grid summarizing DDX20 immunohistochemical staining data from 70 cases. In 47 cases (pink shading), DDX20 protein levels were lower in the HCC tissues than in the surrounding tissues ($P < 0.05$; Wilcoxon signed-rank test).

confirmed that DDX20 expression was frequently lower in HCC than in surrounding noncancerous liver tissue (Fig. 1C,D). Specifically, 47 of 70 cases examined showed reduced DDX20 protein expression in HCC versus background noncancerous liver tissue (Fig. 1D and Supporting Table 1). These results indicate that the expression of DDX20, an miRNP component, is frequently reduced in human HCC, and suggest that this reduced DDX20 expression might be involved in the pathogenesis of a subset of HCC cases.

***NF-κB Activity Is Enhanced by DDX20 Deficiency.*** Because DDX20 knockout mice are embryonic-lethal,[28] DDX20 has been suggested to have important biological roles. DDX20, a DEAD-box protein,[29] was originally found to interact with survival motor neuron protein.[30] Later, it was identified as a major component of miRNPs,[31] which may mediate miRNA function. As we have reported, DDX20 is preferentially involved in miRNA-140-3p function,[23] acting as a suppressor of NF-κB activity in the liver.[32] DDX20-knockdown PLC/PRF/5 cells exhibit enhanced NF-κB activity[23] (Fig. 2A). Whereas the proliferation rates of DDX20-knockdown cells and control cells were comparable (Fig. 2B), apoptotic cell death after stimulation with TNF-related apoptosis-inducing ligand (TRAIL), which induces both cell apoptosis and NF-κB activation,[33] was significantly reduced in DDX20-knockdown cells (Fig. 2C). Similar results were obtained using DDX20-knockdown HepG2 cells (Supporting Fig. 2A-D). Conversely, NF-κB activity was reduced, but cell proliferation remained unchanged, in Hep3B cells stably overexpressing DDX20 (Fig. 2D,E). Sensitivity to TRAIL-induced apoptosis was restored in these cells (Fig. 2F). Similar results were also obtained using Huh7 cells (Supporting Fig. 2E-H). These data confirm a previous report that DDX20 deficiency enhances NF-κB activity and the downstream events of this pathway.

***Metallothionein Expression Is Decreased by DDX20 Deficiency.*** Next, to investigate the biological consequences of DDX20 deficiency, we examined the changes in transcript levels in DDX20-knockdown cells using microarrays (GEO accession number: GSE28088). The expression of genes driven by NF-κB that are related to carcinogenesis, such as FASLG, IRAK1, CARD9, and Galectin-1, were enhanced significantly in DDX20-knockdown cells, as expected (Table 2). To determine the mechanism underlying the enhanced NF-κB activation in DDX20-deficient cells, we searched for candidate genes and noticed that the

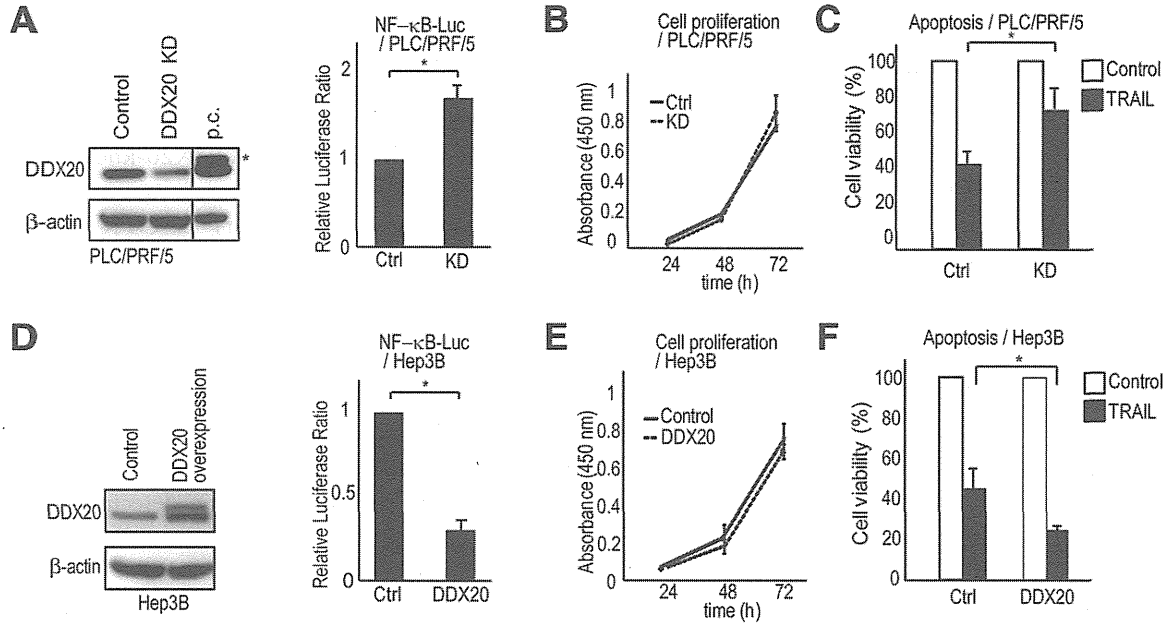


Fig. 2. Modulation of downstream events of the nuclear factor-κB pathway by DDX20. (A) Left: Establishment of stable DDX20-knockdown (DDX20 KD) PLC/PRF/5 cells. *Positive control (p.c.). Right: DDX20 deficiency enhances TNF-α–induced NF-κB activity. NF-κB reporter plasmids were transiently transfected into control (Ctrl) or DDX20-knockdown (KD) PLC/PRF/5 cells. The cells were then treated with TNF-α (5 ng/mL) or vehicle for 6 hours. $*P < 0.05$. Data are presented as the mean ± SD of three independent determinations. (B) Cell proliferation rates were comparable for control (Ctrl) and DDX20-knockdown (KD) PLC/PRF/5 cells. Data are presented as the mean ± SD of three determinations. (C) DDX20 deficiency reduces TRAIL-induced apoptotic cell death. Control (Ctrl) and DDX20-knockdown (KD) PLC/PRF/5 cells were incubated with 25 ng/mL TRAIL. Data represent cell viability after TRAIL stimulation (gray bars) relative to the number of vehicle-treated cells (white bars). $*P < 0.05$. Data are presented as the mean ± SD of triplicate determinations. (D) Left: Establishment of stable DDX20-overexpressing cells. Hep3B cells were infected with control or FLAG-tagged DDX20-overexpressing lentiviruses and selected on puromycin. Western blot analysis confirmed increased expression of DDX20 protein. Right: DDX20 overexpression suppresses TNF-α–induced NF-κB activity. NF-κB reporter plasmids were transiently transfected into Hep3B control (Ctrl) and DDX20-overexpressing (DDX20) cells treated with TNF-α for 6 hours. Data are presented as the mean ± SD of three independent determinations. $*P < 0.05$. (E) Proliferation of control (Ctrl) and DDX20-overexpressing (DDX20) Hep3B cells was measured as described in (B). (F) DDX20 overexpression reduces TRAIL-induced apoptotic cell death. Data for control (Ctrl) and DDX20-overexpressing (DDX20) Hep3B cells are shown. $*P < 0.05$.

**Table 2. Increased Expression of NF-κB–Related Genes in DDX20-Knockdown HepG2 Cells Compared with Wild-Type Cells**

| RefSeq ID | Symbol | Description | Ratio | Representative Gene Function |
|---|---|---|---|---|
| NM_000639 | FASLG | Fas ligand | 3.5 | NF-κB target, apoptosis |
| NM_052813 | C9orf151 | CARD9 | 2.5 | NF-κB cascade, NF-κB target |
| NM_014959 | CARD8 | Tumor up-regulated CARD-containing antagonist of CASP9 (TUCAN) | 2.2 | NF-κB target |
| NM_131917 | FAF1 | FAS-associated factor 1 (hFAF1) | 1.9 | Cytoplasmic sequestering of NF-κB, NF-κB target |
| NM_020644 | TMEM9B | Transmembrane protein 9B precursor | 1.9 | Positive regulation of NF-κB transcription factor activity |
| NM_017544 | NKRF | ITBA4 protein | 1.9 | Negative regulation of transcription |
| NM_006247 | PPP5C | Protein phosphatase T | 1.8 | Positive regulation of NF-κB cascade |
| NM_020345 | NKIRAS1 | KappaB-Ras1 | 1.8 | NF-κB cascade |
| NM_001569 | IRAK1 | IRAK-1 | 1.7 | Positive regulation of NF-κB transcription factor activity |
| NM_177951 | PPM1A | Protein phosphatase 1A | 1.7 | Positive regulation of NF-κB cascade |
| NM_018098 | ECT2 | Epithelial cell-transforming sequence 2 oncogene | 1.6 | Positive regulation of NF-κB cascade |
| NM_002305 | LGALS1 | Galectin-1 (putative MAPK-activating protein MP12) | 1.6 | Positive regulation of NF-κB cascade |
| NM_015093 | TAB2 | TAK1-binding protein 2 | 1.6 | Positive regulation of NF-κB cascade |
| NM_004180 | TANK | TRAF-interacting protein | 1.5 | NF-κB cascade |
| NM_014976 | PDCD11 | Programmed cell death protein 11 | 1.5 | rRNA processing |
| NM_015336 | ZDHHC17 | Putative NF-κB–activating protein 205 | 1.5 | Positive regulation of NF-κB cascade |
| NM_002503 | NFKBIB | IKB-β | 1.5 | Cytoplasmic sequestering of NF-κB |
| NM_138330 | ZNF675 | Zinc finger protein 675 | 1.5 | Negative regulation of NF-κB transcription factor activity |

The genes were identified as NF-κB–related based on the Gene Ontology and the GeneCodis Databases.

**Table 3. Decreased Expression Levels of MT Genes in DDX20 Knockdown HepG2 Cells Compared with Wild-Type Cells**

| Symbol | Description | Ratio |
|---|---|---|
| MT1E | Metallothionein-1E | **0.12** |
| MT1F | Metallothionein-1F | **0.36** |
| MT1H | Metallothionein-1H | **0.16** |
| MT1G | Metallothionein-1G | **0.06** |
| MT1M | Metallothionein-1M | **0.24** |
| MT1X | Metallothionein-1X | **0.27** |
| MT2A | Metallothionein-2 | **0.28** |
| MT3 | Metallothionein-3 | 0.84 |
| MTL5 | Metallothionein-like 5 (Tesmin) | 1.12 |

Numbers in boldface type indicate values <0.5.

expression levels of a group of metallothioneins (MTs), such as MT1E, MT1F, MT1G, MT1M, MT1X, and MT2A, were all significantly decreased when DDX20 was deficient (Table 3). The decreased expression of MTs in DDX20-knockdown HepG2 and PLC/PRF/5 cells was confirmed via quantitative RT-PCR (Fig. 3a and Supporting Fig. 3). Expression of MT-3, which was not altered in the microarray analysis, was similarly unaltered in quantitative RT-PCR analysis. Notably, it was already known that MTs are frequently silenced in human primary liver cancers.[34-36] In addition, MT knockout mice have enhanced NF-κB activity, likely due to reactive oxygen species, and these mice are more prone to hepatocarcinogenesis.[37] These results suggest that DDX20 deficiency enhances NF-κB activity by decreasing the expression of MTs, which could facilitate the development of liver cancer.

***MiRNA-140 Directly Targets Dnmt1.*** Because MT expression is regulated principally by CpG island methylation in their promoter regions,[38,39] we examined the quantitative methylation status of MT promoters in DDX20-knockdown cells. The CpG islands of the MT1E, MT1G, MT1M, MT1X, and MT2A promoters, and the CpG shores of the MT1F promoters, were significantly more highly methylated under DDX20-deficient conditions, as determined by the comprehensive Illumina Quantitative Methylation BeadChip method (Table 4, Supporting Table 2, and GSE 37633). A crucial step in DNA methylation involves DNA methyltransferase (Dnmt), which catalyzes the methylation of CpG dinucleotides in genomic DNA.[40] The methylation status of MT promoters is mediated specifically by Dnmt1.[41] Because Dnmt1 contains a predicted miRNA-140-3p target site in its 3′ UTR, with a perfect match to its seed sequences (Fig. 3B), and because the effects of miRNA-140-3p activity were impaired in DDX20-knockdown cells,[23] it was hypothesized that whereas miRNA-140 normally targets and suppresses Dnmt1 protein expression, miRNA-140-3p dysfunction due to DDX20 deficiency results in enhanced Dnmt1 expression, leading to hypermethylation of MT promoters. Consistent with this hypothesis, Dnmt1 expression was increased significantly in DDX20-knockdown cells (Fig. 3C). miRNA-140 precursor overexpression suppressed activity of the Dnmt1 3′ UTR reporter construct, the effect of which was lost when two mutations were introduced into its seed sequences (Fig. 3D). MiRNA-140 precursor overexpression suppressed Dnmt1 protein expression (Fig. 3E). These results indicate that miRNA-140 directly targets Dnmt1 and suppresses its expression in the normal state. Consistently, decreased DDX20, increased Dnmt1, and decreased MT expression were detected together in human clinical HCC samples, as determined via immunohistochemistry (Fig. 3F). By contrast, miRNA-140 precursor-overexpressing Huh7 cells showed increased expression of MTs and reduced NF-κB activity *in vitro* (Supporting Fig. 4A,B). Moreover, the increase in the number of spheres formed from PLC/PRF/5 cells due to DDX20 knockdown was antagonized by treatment with an NF-κB inhibitor or a demethylating agent (Supporting Fig. 5). Taken together, these results suggest that the up-regulated Dnmt1 protein expression caused by functional impairment of miRNA-140-3p due to DDX20 deficiency results in decreased expression of MTs *via* enhanced methylation at the CpG sites in their promoters. This may lead to enhanced NF-κB activity and cellular transformation at least *in vitro*.

***MiRNA-140 Is a Liver Tumor Suppressor.*** To further examine the biological consequences of functional impairment of miRNA-140 due to DDX20 deficiency, we determined the phenotypes of miRNA-140 knockout (miRNA-140$^{-/-}$) mice (Fig. 4A). Similar to the *in vitro* DDX20 knockdown results, Dnmt1 expression was increased and MT levels decreased in the liver tissue of these mice (Fig. 4B). NF-κB–DNA binding activity was enhanced in the livers of miRNA-140$^{-/-}$ mice after tail-vein injection of TNF-α, a crucial cytokine that induces NF-κB activity and hepatocarcinogenesis (Fig. 4C). As was found in MT knockout mice, phosphorylation of p65 at serine 276, which is critical for p65 activation, was significantly increased in the livers of miRNA-140$^{-/-}$ mice after DEN exposure, which induces NF-κB activation and liver tumors[37] (Fig. 4D). Notably, the size and number of liver tumors that developed 8 months after DEN exposure were markedly elevated in miRNA-140$^{-/-}$ mice compared with control mice (Fig. 4E,F). These results indicate that miRNA-140$^{-/-}$ mice are indeed

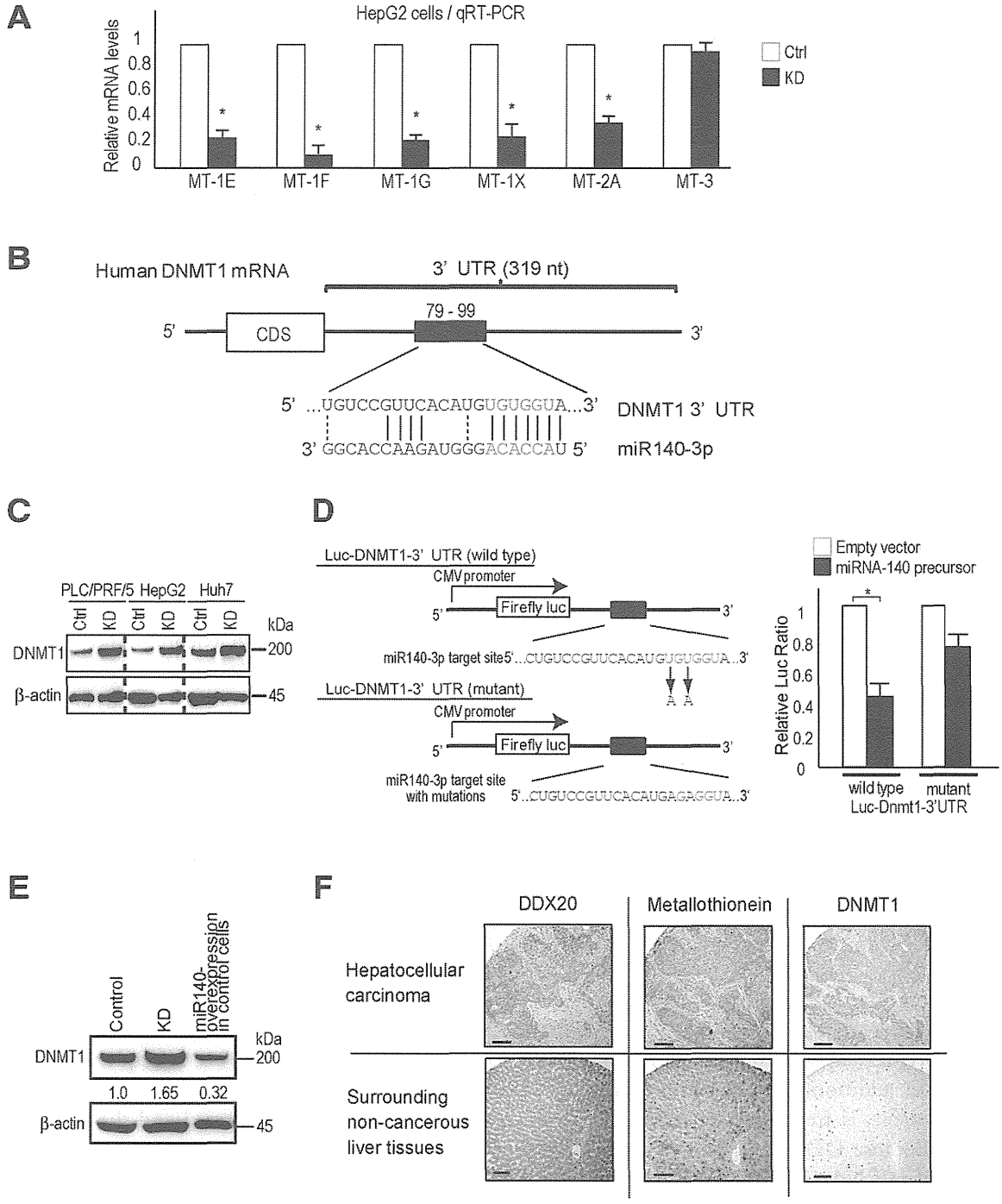


Fig. 3. Targeting of Dnmt1 by miRNA-140-3p and reduced MT expression. (A) The expression levels of MTs were determined using quantitative reverse-transcriptase polymerase chain reaction. The relative expression ratios of the MTs in control (white bars) and DDX20-knockdown (black bars) HepG2 cells were calculated by normalizing control cell values to 1.0. The data represent the mean ± SD of three independent determinations. $*P < 0.05$. (B) Putative miRNA-140-3p target sites in the 3′ UTR of human Dnmt1. Seed sequences are indicated in red. (C) Dnmt1 expression was increased in DDX20-knockdown cells. Ctrl, control cells; KD, DDX20-knockdown cells. (D) Left: Schematic diagrams of wild-type (upper) and mutant (lower) luciferase reporter constructs (Luc-Dnmt1-3′ UTRs) carrying the Dnmt1 3′ UTR region harboring the putative miRNA-140-3p target site. The mutant seed sequence contained two nucleotide substitutions. Right: The Dnmt1 3′ UTR is targeted directly by miRNA-140-3p. Cells were cotransfected with Luc-Dnmt1-3′ UTR (wild-type or mutant) plus either an empty vector (white bars) or a plasmid expressing the miRNA-140 precursor (black bars). Data are the mean ± SD of three independent determinations. (E) Overexpression of miRNA-140 reduces Dnmt1 expression in control cells. Values between the panels indicate Dnmt1 protein levels normalized to those of β-actin. KD, DDX20 knockdown cells. (F) Representative histochemical images showing expression of DDX20, Dnmt1, and MT proteins in HCC (upper three panels) and surrounding tissue (lower panels). Compared with adjacent noncancerous liver tissue, HCCs exhibited decreased DDX20 and MT expression and increased Dnmt1 expression. Note that adjacent sections were stained for each protein. Scale bar, 50 μm.

**Table 4. Methylation Levels in CpG Islands of the MT Genes in DDX20-Knockdown HepG2 Cells Compared with Control Cells**

| Symbol | CpG Island Methylation Ratio | Target ID |
|---|---|---|
| MT1E | **1.14** | cg00178359 |
| | **1.29** | cg06463589 |
| | **3.65** | cg02512505 |
| | **1.02** | cg15134649 |
| MT1G | **2.14** | cg16452857 |
| | **1.03** | cg27367960 |
| | 1.00 | cg03566142 |
| | 0.99 | cg07791866 |
| MT1M | **1.16** | cg02132560 |
| | 0.98 | cg02160530 |
| | **1.03** | cg04994964 |
| MT1X | **1.24** | cg05596720 |
| | **1.05** | cg26802333 |
| | **1.06** | cg09147880 |
| | **1.01** | cg08872713 |
| MT2A | **2.06** | cg07395075 |
| | 0.94 | cg20430434 |

Values were determined using the quantitative Illumina Human Methylation BeadsChip. Boldface values indicate increased methylation levels in DDX20 knockdown cells.

more prone to liver cancer development and suggest that miRNA-140 acts as a liver tumor suppressor, probably by suppressing NF-κB activity, although we cannot completely exclude other molecular mechanisms. Nonetheless, these results also suggest that the impairment of miRNA-140 function due to DDX20 deficiency may lead to hepatocarcinogenesis in humans, as we have observed in miRNA-140$^{-/-}$ mice (Supporting Figs. 6 and 7).

## Discussion

Here, we report that miRNA-140$^{-/-}$ mice have increased NF-κB activity and are more prone to HCC development. In addition, we show that DDX20, an miRNP component, is frequently decreased in human HCC tissues. Because DDX20 deficiency preferentially causes impaired miRNA-140 function,[23] the functional impairment of miRNA-140 may result in phenotypes similar to those of miRNA-140$^{-/-}$ mice and may lead to hepatocarcinogenesis. In support of the hypothesis that DDX20 dysfunction is involved in hepatocarcinogenesis, DDX20 is located at 1p21.1-p13.2, a frequently deleted chromosomal region in human HCC,[27] and DDX20 was recently identified as a possible liver tumor suppressor in a functional screen in mice.[27] Although the possibility that intracellular signaling pathways other than miRNA-140 may also be involved in the biological consequences of DDX20 deficiency cannot be denied, we believe that functional impairment of miRNA-140 plays a major role in the phenotypes induced by DDX20 deficiency, based on the phenotypic similarities.

Changes in miRNA expression levels have been reported in various tumors.[7,12,42] However, in this study, we found that reduced expression of an miRNA machinery component might lead to carcinogenesis, at least in part, through functional impairment of miRNAs. Recent studies have shown that components of the RNA interference machinery are associated with the outcome of ovarian cancer patients,[43] and that single-nucleotide polymorphisms in miRNA machinery genes can be used as diagnostic risk markers.[44,45] Therefore, the impairment of miRNA function caused by deregulated miRNA machinery components may also be involved in carcinogenesis.

Our study identified Dnmt1 as a critical target of miRNA-140. The decreased MT expression due to the CpG promoter methylation induced by Dnmt1 resulted in enhanced NF-κB activity. This finding was consistent with the results obtained using MT gene knockout mice, in which enhanced NF-κB activation promoted hepatocarcinogenesis.[37] The decrease in MT expression that results from increased Dnmt1 expression caused by functional impairment of miRNA-140, together with increased NF-κB activation and hepatocarcinogenesis in MT knockout mice,[37] supports the concept that the DDX20/miRNA-140/Dnmt1/MT/NF-κB pathway may play a crucial role in hepatocarcinogenesis. However, we cannot fully exclude the possibility that other intracellular signaling pathways are also involved in the induction of hepatocarcinogenesis by miRNA-140 or DDX20 deficiency, because the precise role of NF-κB in hepatocarcinogenesis has not been clearly defined,[8] although constitutive activation of NF-κB signaling has been frequently detected in human HCCs.[46] The mechanisms by which DDX20 expression is initially decreased and the reason its locus is frequently deleted in HCC remain to be elucidated. However, because DDX20 expression is also regulated by methylation of its CpG promoter,[47] once this pathway is deregulated, decreased DDX20 expression could be maintained by a positive feedback mechanism, even without deletion of its locus.[27]

In conclusion, this study shows that miRNA-140 acts as a liver tumor suppressor. We show that DDX20, an miRNP component, is frequently decreased in human HCC, which may induce hepatocarcinogenesis via impairment of miRNA-140 function. These results suggest the importance of investigations of not only aberrant miRNA expression levels,[12,14,17,48] but also deregulation of miRNP

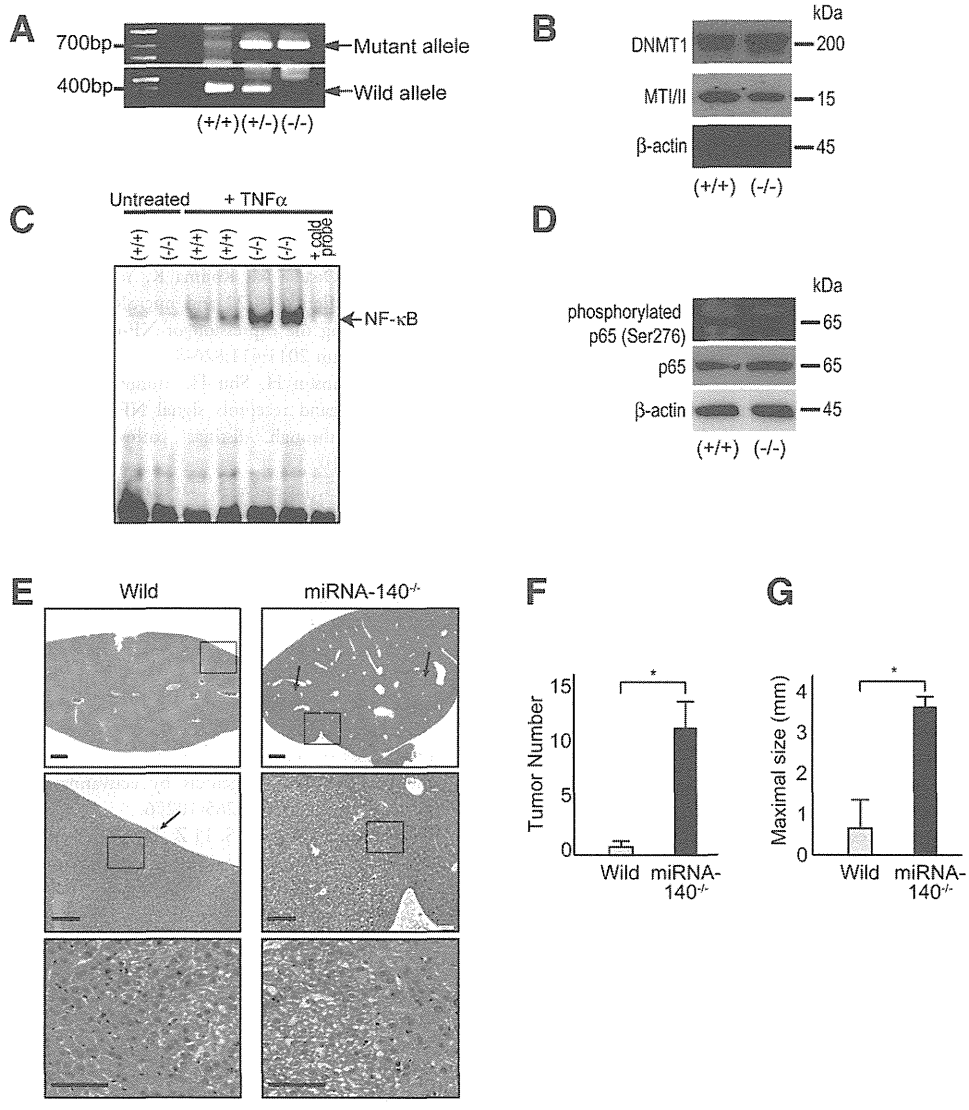


Fig. 4. miRNA-140$^{-/-}$ mice are prone to hepatocarcinogenesis. (A) Representative genotyping of mice with wild-type or mutant alleles. PCR genotyping was performed for miRNA-140 wild-type (419 bp; Wild) and knockout (734 bp; Mutant) alleles. (+/+), wild-type; (+/−), heterozygous; (−/−), knockout. (B) Increased Dnmt1 expression and decreased MTI/II expression in the liver tissues of miRNA-140$^{-/-}$ mice compared with wild-type mice. Western blotting was performed using antibodies against the indicated proteins. (+/+), wild-type; (−/−), miRNA-140$^{-/-}$. The image shown is representative of four independent experiments. (C) NF-κB–DNA binding was assessed via gel-shift assay using equal amounts of liver nuclear extracts from untreated and TNF-α–injected wild-type and miRNA-140$^{-/-}$ mice. (+/+), wild-type; (−/−), miRNA-140$^{-/-}$. Cold probe was added to TNF-α–injected knockout mouse nuclear extract to test assay specificity. A result representative of four independent experiments is shown. (D) Western blotting for phosphorylated p65 expression in the liver at 32 weeks after DEN treatment in miRNA-140$^{-/-}$ mice compared with wild-type mice. A result representative of four independent experiments is shown. (E) Representative histological images of mouse liver at 32 weeks after DEN treatment. Arrows indicate tumors. Higher-magnification images of the highlighted areas in the upper panels are shown in the lower panels. Scale bar, 500 μm. (F) The number (left panel) and size (right panel) of tumors (five random sections per mouse treated with DEN) are presented as the mean ± SD (wild-type mice, n = 8; miRNA-140$^{-/-}$ mice, n = 8). *$P < 0.05$.

components,[22] with subsequent impairment of miRNA function as molecular pathways and possible therapeutic targets for carcinogenesis and other diseases.

## References


1. Parkin D, Bray F, Ferlay J, Pisani P. Global cancer statistics, 2002. CA Cancer J Clin 2005;55:74-108.
2. Block T, Mehta A, Fimmel C, Jordan R. Molecular viral oncology of hepatocellular carcinoma. Oncogene 2003;22:5093-5107.
3. Karin M. Nuclear factor-kappaB in cancer development and progression. Nature 2006;441:431-436.
4. Luedde T, Schwabe RF. NF-κB in the liver—linking injury, fibrosis and hepatocellular carcinoma. Nat Rev Gastroenterol Hepatol 2011;8:108-118.
5. Pikarsky E, Porat R, Stein I, Abramovitch R, Amit S, Kasem S, et al. NF-kappaB functions as a tumour promoter in inflammation-associated cancer. Nature 2004;431:461-466.
6. Liu P, Kimmoun E, Legrand A, Sauvanet A, Degott C, Lardeux B, et al. Activation of NF-kappa B, AP-1 and STAT transcription factors is a frequent and early event in human hepatocellular carcinomas. J Hepatol 2002;37:63-71.

7. Ji J, Shi J, Budhu A, Yu Z, Forgues M, Roessler S, et al. MicroRNA expression, survival, and response to interferon in liver cancer. N Engl J Med 2009;361:1437-1447.
8. Feng GS. Conflicting roles of molecules in hepatocarcinogenesis: paradigm or paradox. Cancer Cell 2012;21:150-154.
9. Bartel DP. MicroRNAs: target recognition and regulatory functions. Cell 2009;136:215-233.
10. Otsuka M, Jing Q, Georgel P, New L, Chen J, Mols J, et al. Hypersusceptibility to vesicular stomatitis virus infection in Dicer1-deficient mice is due to impaired miR24 and miR93 expression. Immunity 2007;27:123-134.
11. Otsuka M, Zheng M, Hayashi M, Lee JD, Yoshino O, Lin S, et al. Impaired microRNA processing causes corpus luteum insufficiency and infertility in mice. J Clin Invest 2008;118:1944-1954.
12. Kojima K, Takata A, Vadnais C, Otsuka M, Yoshikawa T, Akanuma M, et al. MicroRNA122 is a key regulator of α-fetoprotein expression and influences the aggressiveness of hepatocellular carcinoma. Nat Commun 2011;2:338.
13. Chang T-C, Yu D, Lee Y-S, Wentzel EA, Arking DE, West KM, et al. Widespread microRNA repression by Myc contributes to tumorigenesis. Nat Genet 2008;40:43-50.
14. Lu J, Getz G, Miska EA, Alvarez-Saavedra E, Lamb J, Peck D, et al. MicroRNA expression profiles classify human cancers. Nature 2005; 435:834-838.
15. Calin GA, Croce CM. MicroRNA signatures in human cancers. Nat Rev Cancer 2006;6:857-866.
16. Gaur A, Jewell DA, Liang Y, Ridzon D, Moore JH, Chen C, et al. Characterization of microRNA expression levels and their biological correlates in human cancer cell lines. Cancer Res 2007;67:2456-2468.
17. Kumar MS, Lu J, Mercer KL, Golub TR, Jacks T. Impaired microRNA processing enhances cellular transformation and tumorigenesis. Nat Genet 2007;39:673-677.
18. Lambertz I, Nittner D, Mestdagh P, Denecker G, Vandesompele J, Dyer MA, et al. Monoallelic but not biallelic loss of Dicer1 promotes tumorigenesis in vivo. Cell Death Differ 2010;17:633-641.
19. Otsuka M, Takata A, Yoshikawa T, Kojima K, Kishikawa T, Shibata C, et al. Receptor for activated protein kinase C: requirement for efficient microRNA function and reduced expression in hepatocellular carcinoma. PLoS One 2011;6:e24359.
20. Lujambio A, Esteller M. CpG island hypermethylation of tumor suppressor microRNAs in human cancer. Cell Cycle 2007;6:1455-1459.
21. Thomson J, Newman M, Parker J, Morin-Kensicki E, Wright T, Hammond S. Extensive post-transcriptional regulation of microRNAs and its implications for cancer. Genes Dev 2006;20:2202-2207.
22. Melo SA, Ropero S, Moutinho C, Aaltonen LA, Yamamoto H, Calin GA, et al. A TARBP2 mutation in human cancer impairs microRNA processing and DICER1 function. Nat Genet 2009;41:365-370.
23. Takata A, Otsuka M, Yoshikawa T, Kishikawa T, Kudo Y, Goto T, et al. A miRNA machinery component DDX20 controls NF-κB via microRNA-140 function. Biochem Biophys Res Commun 2012;13:564-569.
24. Miyaki S, Sato T, Inoue A, Otsuki S, Ito Y, Yokoyama S, et al. MicroRNA-140 plays dual roles in both cartilage development and homeostasis. Genes Dev 2010;24:1173-1185.
25. Garzon R, Heaphy CE, Havelange V, Fabbri M, Volinia S, Tsao T, et al. MicroRNA 29b functions in acute myeloid leukemia. Blood 2009;114:5331-5341.
26. Mourelatos Z, Dostie J, Paushkin S, Sharma A, Charroux B, Abel L, et al. miRNPs: a novel class of ribonucleoproteins containing numerous microRNAs. Genes Dev 2002;16:720-728.
27. Zender L, Xue W, Zuber J, Semighini C, Krasnitz A, Ma B, et al. An oncogenomics-based in vivo RNAi screen identifies tumor suppressors in liver cancer. Cell 2008;135:852-864.
28. Mouillet J, Yan X, Ou Q, Jin L, Muglia L, Crawford P, et al. DEAD-box protein-103 (DP103, Ddx20) is essential for early embryonic development and modulates ovarian morphology and function. Endocrinology 2008;149:2168-2175.
29. Voss M, Hille A, Barth S, Spurk A, Hennrich F, Holzer D, et al. Functional cooperation of Epstein-Barr virus nuclear antigen 2 and the survival motor neuron protein in transactivation of the viral LMP1 promoter. J Virol 2001;75:11781-11790.
30. Charroux B, Pellizzoni L, Perkinson R, Shevchenko A, Mann M, Dreyfuss G. Gemin3: a novel DEAD box protein that interacts with SMN, the spinal muscular atrophy gene product, and is a component of gems. J Cell Biol 1999;147:1181-1194.
31. Hutvágner G, Zamore P. A microRNA in a multiple-turnover RNAi enzyme complex. Science 2002;297:2056-2060.
32. Takata A, Otsuka M, Kojima K, Yoshikawa T, Kishikawa T, Yoshida H, et al. MicroRNA-22 and microRNA-140 suppress NF-κB activity by regulating the expression of NF-κB coactivators. Biochem Biophys Res Commun 2011;411:826-831.
33. Hu W, Johnson H, Shu H. Tumor necrosis factor-related apoptosis-inducing ligand receptors signal NF-kappaB and JNK activation and apoptosis through distinct pathways. J Biol Chem 1999;274: 30603-30610.
34. Cherian MG, Jayasurya A, Bay BH. Metallothioneins in human tumors and potential roles in carcinogenesis. Mutat Res 2003;533:201-209.
35. Huang GW, Yang LY. Metallothionein expression in hepatocellular carcinoma. World J Gastroenterol 2002;8:650-653.
36. Datta J, Majumder S, Kutay H, Motiwala T, Frankel W, Costa R, et al. Metallothionein expression is suppressed in primary human hepatocellular carcinomas and is mediated through inactivation of CCAAT/enhancer binding protein alpha by phosphatidylinositol 3-kinase signaling cascade. Cancer Res 2007;67:2736-2746.
37. Majumder S, Roy S, Kaffenberger T, Wang B, Costinean S, Frankel W, et al. Loss of metallothionein predisposes mice to diethylnitrosamine-induced hepatocarcinogenesis by activating NF-kappaB target genes. Cancer Res 2010;70:10265-10276.
38. Ghoshal K, Majumder S, Li Z, Dong X, Jacob ST. Suppression of metallothionein gene expression in a rat hepatoma because of promoter-specific DNA methylation. J Biol Chem 2000;275:539-547.
39. Harrington MA, Jones PA, Imagawa M, Karin M. Cytosine methylation does not affect binding of transcription factor Sp1. Proc Natl Acad Sci U S A 1988;85:2066-2070.
40. Li E, Beard C, Jaenisch R. Role for DNA methylation in genomic imprinting. Nature 1993;366:362-365.
41. Majumder S, Kutay H, Datta J, Summers D, Jacob ST, Ghoshal K. Epigenetic regulation of metallothionein-i gene expression: differential regulation of methylated and unmethylated promoters by DNA methyltransferases and methyl CpG binding proteins. J Cell Biochem 2006; 97:1300-1316.
42. Garzon R, Calin G, Croce C. MicroRNAs in cancer. Annu Rev Med 2009;60:167-179.
43. Merritt W, Lin Y, Han L, Kamat A, Spannuth W, Schmandt R, et al. Dicer, Drosha, and outcomes in patients with ovarian cancer. N Engl J Med 2008;359:2641-2650.
44. Horikawa Y, Wood CG, Yang H, Zhao H, Ye Y, Gu J, et al. Single nucleotide polymorphisms of microRNA machinery genes modify the risk of renal cell carcinoma. Clin Cancer Res 2008;14:7956-7962.
45. Yang H, Dinney CP, Ye Y, Zhu Y, Grossman HB, Wu X. Evaluation of genetic variants in microRNA-related genes and risk of bladder cancer. Cancer Res 2008;68:2530-2537.
46. Wu JM, Sheng H, Saxena R, Skill NJ, Bhat-Nakshatri P, Yu M, et al. NF-kappaB inhibition in human hepatocellular carcinoma and its potential as adjunct to sorafenib based therapy. Cancer Lett 2009;278: 145-155.
47. Gebhard C, Schwarzfischer L, Pham T, Andreesen R, Mackensen A, Rehli M. Rapid and sensitive detection of CpG-methylation using methyl-binding (MB)-PCR. Nucleic Acids Res 2006;34:e82.
48. Martello G, Rosato A, Ferrari F, Manfrin A, Cordenonsi M, Dupont S, et al. A microRNA targeting dicer for metastasis control. Cell 2010; 141:1195-1207.